OCEAN DRILLING PROGRAM

LEG 165 PRELIMINARY REPORT

CARIBBEAN OCEAN HISTORY AND

THE CRETACEOUS/TERTIARY BOUNDARY EVENT

Dr. Haraldur Sigurdsson
Co-Chief Scientist, Leg 165
Graduate School of Oceanography
University of Rhode Island
Narragansett, Rhode Island 02828
U.S.A.

Dr R. Mark Leckie
Co-Chief Scientist, Leg 165
Department of Geosciences
University of Massachusetts
Amherst, Massachusetts 01003
U.S.A.

Dr. Gary D. Acton
Staff Scientist, Leg 165
Ocean Drilling Program
Texas A&M University Research Park
1000 Discovery Drive
College Station, TX 77845-9547
U.S.A.

Paul J. Fox
Director, Science Operations
ODP/TAMU

Jack Baldauf
Manager, Science Operations
ODP/TAMU

Timothy J. G. Francis
Deputy Director
ODP/TAMU

March 1996

Preliminary Report No. 65

First Printing 1996

Distribution

Electronic copies of this report can be found on the ODP Publications Home Page on the World Wide Web at http://www-odp.tamu.edu/publications.

SCIENTIFIC REPORT

The following scientists were aboard JOIDES Resolution for Leg 165 of the Ocean Drilling Program:

Haraldur Sigurdsson, Co-Chief Scientist (Graduate School of Oceanography, University of Rhode Island, Narragansett, Rhode Island 02882-1197, USA, E-mail: haraldur@gsosun1.gso.uri.edu)
Mark Leckie, Co-Chief Scientist (Department of Geosciences, University of Massachusetts, Amherst, Massachusetts 01003, USA, E-mail: mleckie@eclogite.geo.umass.edu)
Gary D. Acton, Staff Scientist (Ocean Drilling Program, Texas A&M Research Park, 1000 Discovery Drive, College Station, Texas 77845-9547, USA, E-mail: gary_acton@odp.tamu.edu)
Lewis J. Abrams, JOIDES Logger (Department of Geology, University of Puerto Rico, P.O. Box 5000, Mayaguez, Puerto Rico 00681-5000, E-mail: lew@bigwave.upr.clu.edu)
Timothy J. Bralower, Paleontologist (Nannofossils) (Department of Geology, University of North Carolina, Chapel Hill, North Carolina 27599-3315, USA, E-mail: tjbralow@email.unc.edu)
Steven N. Carey, Sedimentologist (Graduate School of Oceanography, University of Rhode Island, South Ferry Road, Narragansett, Rhode Island 02882-1197, USA, E-mail: scarey@gsosun1.gso.uri.edu)
William P. Chaisson, Paleontologist (Foraminifers) (Paleontological Research Institution, 1259 Trumansburg Road, Ithaca, New York 14850, USA, E-mail: 71024.617@compuserve.com)
Pierre Cotillon, Sedimentologist (Université Lyon I, Centre des Sciences de la Terre, 43 Boulevard du 11 novembre, 69622 Villeurbanne Cedex, France)
Andrew Cunningham, Physical Properties Specialist (Department of Geology and Geophysics, Rice University, MS-126, 6100 South Main, Houston, Texas 77005-1892, USA, E-mail: andyc@geophysics.rice.edu)
Steven L. D'Hondt, Paleontologist (Foraminifers) (Graduate School of Oceanography, University of Rhode Island, Narragansett Bay Campus, Narragansett, Rhode Island 02882, USA, E-mail: dhondt@gsosun1.gso.uri.edu)
André Droxler, Sedimentologist (Department of Geology and Geophysics, MS-126, Rice University, P.O. Box 1892, Houston, Texas 77251, USA, E-mail: andre@ruf.rice.edu)
Bruno Galbrun, Paleomagnetist (Département de Géologie Sédimentaire, Université Pierre et Marie Curie, Case 117, 4 Place Jussieu, F75252 Paris Cedex 05, France, E-mail: bgalbrun@ccr.jussieu.fr)
Juan Gonzalez, Observer (Colombia)/Sedimentologist (INGEOMINAS, Cali, A.A. 9724, Colombia, E-mail: uocali@mafalda.univalle.edu.co)
Gerald Haug, Sedimentologist (GEOMAR, Wischhofstrasse 1-3, D-24148 Kiel, Germany, E-mail: ghaug@geomar.de)
Koji Kameo, Paleontologist (Nannofossils) (Technical Research Center, Teikoku Oil Co., Ltd., 9-23-30, Kita-karasuyama, Setagayaku, Tokyo 157, Japan, E-mail: vyqO1434@niftyserve.or.jp)
John King, Paleomagnetist (Graduate School of Oceanography, University of Rhode Island, South Ferry Road, Narragansett, Rhode Island 02882-1197, USA, E-mail: jking@gsosun1.gso.uri.edu)

Ida L. Lind, Physical Properties Specialist (Danmarks Tekniske Universitet, Institut for Geologi og Geoteknik, Bygning 204, DK-2800 Lyngby, Denmark, E-mail: iggil@unidhp.uni-c.dk)
Véronique Louvel, LDEO Logger (Laboratoire de Mesures en Forage (ODP), Institut Mediterranéen de Technologie, Technopole de Château Gombert, 13451 Marseille Cedex 20, France, E-mail: louvel@imtmer1.imt-mrs.fr)
Timothy W. Lyons, Organic Geochemist (Department of Geological Sciences, University of Missouri, Columbia, 101 Geological Sciences Building, Columbia, Missouri 65211, USA, E-mail: geoltl@showme.missouri.edu)
Richard W. Murray, Inorganic Geochemist (Department of Earth Sciences, Boston University, Boston, Massachusetts 02215, USA, E-mail: rmurray@bu.edu)
Maria Mutti, Sedimentologist (Geological Institute, Swiss Federal Institute of Technology, Sonneggstrasse 5, CH-8092 Zürich, Switzerland, E-mail: maria@erdw.ethz.ch)
Greg Myers, LDEO Trainee (Borehole Research Group, Lamont-Doherty Earth Observatory, Palisades, New York 10964, USA, E-mail: gmyers@ldeo.columbia.edu)
Richard B. Pearce, Sedimentologist (Department of Oceanography, University of Southampton, Southampton Oceanography Centre, Waterfront Campus, European Way, Southampton SO14 3ZH, E-mail: rbp@soton.ac.uk)
D. Graham Pearson, Inorganic Geochemist (Department of Geological Sciences, Durham University, South Road, Durham DH1 3LE, United Kingdom, E-mail: d.g.pearson@durham.ac.uk)
Larry C. Peterson, Sedimentologist (Rosenstiel School of Marine & Atmospheric Science, University of Miami, 4600 Rickenbacker Causeway, Miami, Florida 33149-1098, USA, E-mail: petersonl@rcf.rsmas.miami.edu)
Ursula Röhl, Physical Properties Specialist (Fachbereich Geowissenschaften, Bremen University, P.O. Box 33 04 40, D-28334 Bremen, Germany, E-mail: uroehl@allgeo.uni-bremen.de)

Observers

Katherine Ellins, Observer, JOIDES Office (JOIDES Office, University of Wales, College of Cardiff, Cardiff, CF1 3YE, United Kingdom)
Maria Gabriela Pineda Occhiena, Observer, Honduras (Direccion General de Pesca y Acuicultura, Departamento de Investigacion y Tecnologia, Ministerio de Recursos Naturales, Boulevard Mira Flores, Avenida La Fao, Tegucigalpa, Honduras)
Jaime Bonilla, Observer, Venezuela (Instituto Oceanográfico de Venezuela, Departamento de Oceanografía, Av. Universidad Cerro Colorado, Cumana, Edo Sucre, Venezuela)
Irene Truskowski Observer, Venezuela (Exploration Maraven SA, Apdo. 829, Caracas 1010A, Venezuela, Email: epxg16@bioserv.maraven.pdv.com)

ABSTRACT

The Cretaceous/Tertiary (K/T) and ocean history goals of ODP Leg 165 were accomplished through drilling at five sites. Highlights of the leg included the recovery of K/T boundary clays and ejecta deposits (at Site 1001 and perhaps Site 999), and the recovery of igneous basement from the Caribbean Oceanic Plateau (Site 1001). Beyond any of our pre-cruise goals or expectations, we discovered a spectacular record of Eocene and Miocene explosive volcanism at Sites 998, 999, 1000, and 1001, which is unmatched in its magnitude and chronostratigraphic resolution. This includes the first documentation of arc volcanism along the Cayman Ridge. Also recorded above the excellently preserved basement/sediment contact in the two holes at Site 1001 is a mid-Campanian volcanic episode, probably the waning stages in the formation of the basaltic plateau that is the foundation of the Caribbean Plate. The age, physical characteristics, and geochemistry of the underlying basalts will bear importantly on the tectonic history of the Caribbean. The vesicularity of the basalts, the benthic microfossils found in sediments resting on the flows, and the magnetic directions recorded by the flows indicate the plateau was rapidly subsiding and near the paleoequator in the mid-Campanian. Geochemical results indicate that dispersed volcanic ash (excluding discrete ash layers) is a significant constituent (typically 10% to 20%) of the Caribbean sedimentary record. The ash alteration products strongly influence the composition of pore waters and may be an important source of silica for the vast accumulation of cherts that abound in the Eocene marine record.

Important paleoceanographic events recovered by drilling include the K/T boundary, the “late Paleocene thermal maximum” (LPTM), and a middle/late minimum in carbonate accumulation (“carbonate crash”). All three holes from which the K/T boundary interval was recovered contained an unusual limestone layer that directly overlies clays and claystone. The limestone, though only a few centimeters thick, is anomalous in that it appears more massive, more indurated, and lighter in color (white to very light gray) than any other limestone recovered during the leg. The LPTM also marks a change in lithology and physical properties, characterized by a faintly laminated claystone unit, less than one meter thick, with significantly lower carbonate content than surrounding chalks and limestones. The spatial distribution of a middle/late Miocene minimum in carbonate accumulation (“carbonate crash”) was extended from a regional anomaly in the Pacific to an interbasinal tropical anomaly. In addition to these anomalies, the transect of sites with

depths ranging from 916 mbsf (Pedro Channel, Site 1000) to 3260 mbsf (Hess Escarpment, Site 1001) and with continuous depositional sequences offers the opportunity to study Neogene water mass history and circulation across the basin. Finally, Site 1002 from the anoxic Cariaco Basin contains a unique tropical counterpart to high latitude ice cores for studies of large and abrupt climate changes in the latest Quaternary.

INTRODUCTION

The Caribbean region poses a wide array of geologic questions, owing to its relatively uncertain plate tectonic evolution, the nature of its largely unsampled oceanic crust or basement, and its important role in global ocean circulation. With the exception of DSDP Site 502, the Caribbean had not been targeted by the Ocean Drilling Program or Deep Sea Drilling Project for more than two decades. A fresh impetus to Caribbean drilling was provided by the recent discovery of a strewn field of unaltered impact glass spherules or tektites in Haiti and Mexico at the Cretaceous/Tertiary boundary, and the identification of their source in the 180 to 300 km-wide Chicxulub impact crater in the Yucatan. Leg 165 drilling was intended to address two major themes: the nature of the Cretaceous/Tertiary boundary (65 Ma) and the influence of tropical seas on global ocean history and climate evolution. In addition, several of the proposed deeper holes held the prospect of reaching basement and, hence, providing new clues to the early formation of the Caribbean Plate. Drilling at five ODP sites (998, 999, 1000, 1001, and 1002; Fig. 1) has provided an excellent marine record representing nearly 80 m.y. of Earth history, but it has also led to the unexpected discovery of several major episodes of explosive volcanism in the Caribbean region, and the recovery of an important succession of submarine basaltic lava flows of the Caribbean Oceanic Plateau.

RESULTS

Site 998

Site 998 is located on the Cayman Rise, between the Yucatan Basin to the north and the Cayman Ridge and Cayman Trough to the south. This site was targeted for recovery of a continuous Cenozoic section to record the evolution of Caribbean ocean circulation, a Cretaceous/Tertiary boundary section relatively proximal to the Chicxulub impact site, and basement. Owing to the thickness of the sedimentary section and the very slow rate of penetration, the two deeper objectives could not be met within the time constraints of the leg.

A largely complete sedimentary section spanning the lower Eocene (nannofossil Zone CP10) to Pleistocene was cored in two holes at Site 998. Hole 998A was APC cored to a depth of 160.8 mbsf (upper Miocene) with 103.1% recovery, and then XCB cored to a depth of 637.6 mbsf with 57.7% recovery. Hole 998A terminated in upper Eocene nannofossil chalk. A free-fall funnel was deployed but was too deeply buried in soft sediment to successfully reenter with the RCB, so a second hole was drilled. Hole 998B was drilled ahead to 567.9 mbsf before resuming coring operations to a total depth of 904.8 mbsf. Recovery with the RCB was very good, with 83.1% of the drilled interval recovered. Hole 998B terminated in lower Eocene calcareous volcaniclastic mixed sedimentary rock.

Four lithologic units were recognized at Site 998 (Fig. 2). Unit I (0.0-94.3 mbsf; Pleistocene-lower Pliocene) consists of nannofossil ooze with foraminifers and clays interbedded with graded foraminiferal ooze and ash layers. Unit II (94.3-161.0 mbsf; basal Pliocene-uppermost middle Miocene) is subdivided into three subunits, all of which have interbedded turbidites and ash layers. The dominant lithologies in Unit II are clayey nannofossil mixed sediment, nannofossil ooze with foraminifers and clays, and clay with nannofossils. Unit III (161.0-766.0 mbsf; middle Miocene-middle Eocene) consists of nannofossil chalks that grade with depth into limestone with clay. The dominant lithologies of Unit IV (766.0-904.8 mbsf; middle Eocene-lower Eocene) are limestone with clay and calcareous volcaniclastic mixed sedimentary rock, with interbedded altered volcanic ash and volcaniclastic turbidites.

A seismic reflection at 5.15 s two-way traveltime is interpreted as acoustic basement, which we suggest is the top of a volcanic arc of unknown age. Based on logging and physical property velocities obtained at the site, the depth to basement is estimated to be 1100-1130 mbsf at the location of Site 998 (Fig. 2). Thus, about 210 m of the sedimentary section above basement was not cored.

Shipboard biostratigraphy and magnetostratigraphy suggest that the cored section is virtually complete. Sedimentation rates averaged 15-24 m/m.y. in the lower Eocene to middle Miocene interval, 8 m/m.y. in the upper Miocene, and nearly 19 m/m.y. for the Pliocene-Pleistocene; the highest rates are recorded for the Oligocene interval of nannofossil chalk where there are fewer turbidites and discrete ash layers. A shipboard magnetostratigraphy was established for the uppermost 200 m of Hole 998A (Pleistocene-middle Miocene) and all of Hole 998B (basal Oligocene-lower Eocene). A strong drill string overprint and the nature of core quality in the middle Miocene-Oligocene XCB cores of Hole 998A contributed to an absence of interpretable paleomagnetic data through the middle part of the cored section at Site 998.

The sedimentary section at Site 998 yielded several unexpected results, including numerous pelagic turbidites (Fig. 3) and thick ash fall deposits in the Miocene, and thinner but much more frequent volcaniclastic turbidites in the lower to middle Eocene (Fig. 4). The bases of these older turbidites consist of foraminifers in a matrix of redeposited volcanic ash. The Miocene ashes are rhyolitic fallout layers, which were probably derived from distant silicic volcanoes in Central America, while the Eocene volcaniclastic turbidites and associated ash falls were derived from a proximal island arc source, probably the nearby Cayman Ridge. More than 500 ash layers were described at Site 998. Turbidite frequency at this site may have been linked closely with spreading activity in the Cayman Trough and strike-slip motion along the fault zone that defines the northern boundary of the Caribbean Plate.

The concentrations of total organic carbon are extremely low in sediments recovered from Holes 998A and 998B, and most measurements were below analytical resolution. Similarly, methane was found to occur at only trace levels, and additional hydrocarbon gases were not observed. The chemical composition of pore waters in the sediments displays a large range that varies systematically with depth and lithology. A downcore decrease in sulfate in the uppermost 50 m of the sediment and increase in Fe are associated with redox conditions typical for deep-marine suboxic diagenesis.

Marked increases in pore-water Ca and Sr with depth most likely are related to dissolution of carbonate and weathering reactions of the volcanic ash and basement. The decrease in Mg with depth likely reflects the alteration of volcanic ashes to tri-octahedral smectite, which creates a sink for Mg, as well as dolomite precipitation. A number of pore water constituents, notably silica, Rb, K, and alkalinity show downcore variations that strongly parallel the abundance trends for the Miocene silicic volcanic ash layers in the sediments, and the peak abundance in these dissolved components is thought to reflect their release during the initial stages of alteration of volcanic glass in the ash layers. The solid phase geochemistry of the sediments reflects the deposition of three principal components at Site 998: biogenic calcium carbonate, terrigenous detrital material, and dispersed volcanic ash. Using refractory elemental ratios such as Ti/Zr as discriminants of terrigenous and volcanic ash sources, we find that terrigenous material represents about 9% to 10% of total sediment, with a marked peak abundance in the top 120 m of the core, where it approaches concentrations of about 15% to 20% (Fig. 5). The total dispersed ash abundance is about 7% in the cored sediment, but shows a peak up to 30% at the 150-m level, where ash fall layers are also most common.

An important discovery at Site 998 is a marked reduction in pelagic carbonate deposition that occurred during the time of the middle/late Miocene boundary interval about 10-12 Ma. This oceanographic event is well developed in upper Miocene sequences of the central and eastern equatorial Pacific but has not been previously documented in the tropical Atlantic or Caribbean Sea (Fig. 6). Tectonic activity associated with the closing of the Central American Seaway during the late Neogene is suspected to have been an important variable in the evolution of Northern Hemisphere climate and ocean circulation. The signature of strong carbonate dissolution on both sides of the present-day Isthmus of Panama has important tectonic and paleoceanographic implications for the cause and extent of the late Miocene “carbonate crash.”

Site 999

Site 999 is located on the Kogi Rise, a previously unnamed bathymetric high in the Colombian Basin. Situated northeast of Mono Rise and southeast of the Hess Escarpment, the crest of the

Kogi Rise lies some 1000 m above the turbidite-laden floor of the Colombian Basin and is isolated by a saddle from sediments originating from the Hess Escarpment. A continuous Upper Cretaceous to Holocene record was anticipated. This section was targeted for tropical paleoceanographic studies including the closure of the Central American Seaway in the mid-Pliocene, as well as an undisturbed Cretaceous/Tertiary (K/T) boundary sequence located relatively proximal to the Chicxulub impact site. With the eventual goal of coring basement and testing the hypothesis of a hot spot origin for the Caribbean oceanic plateau (i.e., a Large Igneous Province), Site 999 was designated a ‘legacy site’ and a reentry cone and casing were installed in Hole 999B for future reoccupation of the site.

A continuous and apparently complete upper Maastrichtian-Pleistocene section was cored at Site 999 (Fig. 7). Hole 999A was APC cored to a depth of 197.6 mbsf (upper Miocene) with 104.6% recovery, and then XCB cored to a depth of 566.1 mbsf with 89.0% recovery. Hole 999A terminated in lower Miocene clayey calcareous chalk. A reentry cone and 62 m of 16-in. casing were jetted into the seafloor before Hole 999B was drilled ahead and casing installed to a depth of 524 m. Coring operations resumed with the RCB at a depth of 543.4 mbsf and terminated in upper Maastrichtian limestone with clay at a depth of 1066.4 mbsf. Recovery with the RCB was good, with 76.1% of the drilled interval recovered.

Mixtures of biogenic ooze, nepheloid clays, and volcanic ash are the primary constituents of the sediments on Kogi Rise. Six lithologic units were recognized at Site 999. Unit I is subdivided into three subunits. Subunit IA (0.0-150.1 mbsf; Pleistocene-lower Pliocene) consists of nannofossil and foraminiferal clayey mixed sediment with scattered interbedded ash layers. Subunit IB (150.1-229.5 mbsf; lower Pliocene-upper Miocene) is similar to Subunit Ia but contains fewer foraminifers, and Subunit IC (229.5-265.1 mbsf; upper Miocene) is further distinguished by the presence of siliceous microfossils. Unit II is subdivided into two subunits: Subunit IIA (265.1-301.8 mbsf; middle/upper Miocene boundary interval) consists of interbedded clay with nannofossils, clayey nannofossil mixed sediment, and common ash layers, and Subunit IIB (301.8-346.9 mbsf; middle Miocene) is similar to Subunit IIA but contains siliceous microfossils and a higher carbonate content. Unit III (346.9-566.1 mbsf; middle to lower Miocene) consists of clayey calcareous chalk with foraminifers and nannofossils, interbedded with abundant ash layers. Unit IV is subdivided into four subunits. Subunit IVA (572.6-644.9 mbsf; lower Miocene-upper Oligocene) consists of clayey calcareous limestone with common thin ash layers, and Subunit IVB (644.9-690.4 mbsf; upper to lower Oligocene) is similar to Subunit IVA but contains more clay. Subunit IVC (690.4-866.2 mbsf; lower Oligocene-middle Eocene) is also a clayey calcareous limestone but contains thicker and more frequent ash layers than Subunits IVA and IVB. Subunit IVD (866.2-887.0 mbsf; middle Eocene) is likewise similar to Subunit IVb but contains more clay. Unit V is subdivided into two subunits: Subunit VA (887.0-1033.4 mbsf; middle Eocene-upper Paleocene) is a clayey calcareous mixed sedimentary rock with some interbedded ash layers, and Subunit VB (1033.4-1049.3 mbsf; lower Paleocene) is a claystone with some interbedded ash layers. Unit VI (1049.3-1066.4 mbsf) consists of basal Paleocene hard light gray limestone and upper Maastrichtian limestone with clay (Fig. 7).

Shipboard biostratigraphy and magnetostratigraphy suggest that the cored section is complete, although the abrupt changes in lithology at the base of the Paleocene may indicate that some of the bedding surfaces recovered in the Cretaceous/Tertiary boundary interval are not conformable or that recovery was incomplete. A comparison of logging records and the cored sediments suggests that a nearly complete boundary sequence was recovered (Fig. 8). The position of the boundary has been constrained by shipboard paleontology to within 10 cm, and extensive shore-based research is planned. The K/T boundary is tentatively placed at the base of a limestone in Section 165-999B-60R-1, 10 cm (1050.2 mbsf).

The middle to upper Eocene and the lower to middle Miocene portions of the section include an unexpectedly large number of rhyolitic volcanic ash layers (>1200), most likely derived from distant silicic volcanic centers in Central America. These ash layers define two major explosive volcanic episodes, also recorded in the sediments at Site 998 on the Cayman Rise (Fig. 4). Volcanic ash layers account for over 4% of the recovered succession. In addition, solid phase geochemistry reveals that the dispersed ash comproses ~18% of the total sediment recovered at Site 999, and that significant amounts of clays in the background sediment are the altered products of volcanic glass (Fig. 5).

The terrigenous component of the sediment has been quantified through an analysis of chromium variation in the bulk sediment. The composition and quantity of this terrigenous sediment may be closely linked to the history of the Magdalena Fan, which has grown in response to the uplift and erosion of the Andean Cordillera. Growth of the submarine fan has been particularly active since the late Miocene, as evidenced by a marked increase in terrigenous mass accumulation rates (1-2 g/cm^2/k.y.) and an increase in detrital clays (Figs. 5 and 9).

Below the middle Eocene ash layers is a series of radiolarian and foraminifer-rich layers, caused by winnowing on the seafloor or by productivity events in the upper water column. In either case, changes in oceanic circulation between the Caribbean and eastern Pacific are suspected, perhaps related to tectonically influenced portals or to sources of deep/intermediate water masses during late Paleocene-early Eocene time. An anomalous band of dark laminated claystone in the uppermost Paleocene of Site 999 may represent an expanded tropical record of the widespread oceanographic warming event that occurred during latest Paleocene time.

The transition from the middle to upper Miocene is distinguished by a sharp reduction in carbonate content and a marked increase in magnetic susceptibility and in terrigenous mass accumulation rates. This interval is correlative to the late Miocene "carbonate crash" of the central and eastern equatorial Pacific, and is also recognized at Site 998 on the Cayman Rise (Fig. 10). Originally thought to be related to tectonically influenced changes in deep water exchange between the Pacific and Atlantic, linkages with changes in thermohaline circulation may be responsible for the widespread "carbonate crash" on both sides of the present-day Isthmus of Panama.

Preliminary evidence for oceanographic changes resulting from the late Neogene closure of the Central American Seaway is found in the planktonic foraminifer record at Site 999. Sinistrally coiled *Neogloboquadrina pachyderma*, normally a polar/subpolar species, is found in significant numbers through the upper Miocene-lower Pliocene interval. The termination of this interval is linked to the cessation of regional upwelling in the southwestern Caribbean with the closure of the seaway.

The upper Maastrichtian through Oligocene section accumulated at rates of approximately 9-14 m/m.y. (2.2-3.6 g/cm^2/k.y.), although the lower Paleocene is characterized by sedimentation rates that average <5 m/m.y (1.2-1.6 g/cm^2/k.y.). A marked rise in sedimentation rates and bulk mass accumulation rates through the lower Miocene (29 m/m.y.; 3.5-6.5 g/cm^2/k.y.) is due in part to the voluminous volcanic ash input. This interval is followed by reduced rates in the middle and upper

Miocene (19 m/m.y.; 1.5-2.5 g/cm^2/k.y.), an interval that includes the "carbonate crash." The Pliocene-Pleistocene interval is characterized by a return to higher sedimentation and mass accumulation rates (30-33 m/m.y.; 2.6-3.4 g/cm^2/k.y.) in response to increased terrigenous input from the northern Andes.

Site 1000

Site 1000 is located in Pedro Channel, one of a series of channels that dissects the carbonate shelves and isolated carbonate banks that define the ENE trending northern Nicaragua Rise (NNR). One of our principal objectives at Site 1000 was to reach the top of a carbonate platform and document the onset of the Caribbean Current. It has been proposed that the NNR was a large carbonate platform during much of the Paleogene that ultimately became segmented due to tectonic activity along the northern Caribbean Plate boundary. Pedro Channel represents one of the largest segments of the once contiguous megabank, originally thought to have foundered during middle Miocene time (Droxler et al., 1992). The carbonate platform proved to be deeper and older than predicted. The thick and continuous 20-m.y. record of pelagic sedimentation cored at Site 1000, however, provides many new insights into the history of Caribbean sub-thermocline (intermediate) water masses, the segmentation and subsidence history of the NNR, the seismic stratigraphy of the region, and a record of explosive volcanism during the Neogene.

A continuous, fairly homogeneous, and apparently complete lower Miocene-Holocene section was cored at Site 1000. Hole 1000A was APC cored to a depth of 312.9 mbsf (middle Miocene) with 103.5% recovery, and then XCB cored to a depth of 553.2 mbsf with 89.2% recovery. Hole 1000A was terminated in middle Miocene calcareous limestone with nannofossils, after coring mainly periplatform oozes and chalks. At Hole 1000B two cores were recovered in oozes above 117 mbsf before the hole was drilled ahead to a depth of 503.5 m with the RCB system. Hole 1000B was terminated in lower Miocene limestone at a depth of 695.9 mbsf with recovery averaging 67.6% over the cored interval.

The 696-m-thick sedimentary sequence recovered in two holes at Site 1000 consists dominantly of periplatform sediments and sedimentary rocks, interbedded with volcanic ash layers and intervals of redeposited periplatform/pelagic and neritic carbonate sediments from the slopes and top of adjacent shallow carbonate banks. Two main lithologic units were recognized based mainly on degree of lithification (Fig. 11); Unit I is a mixture of biogenic and calcareous ooze and chalk, whereas Unit II comprises mixtures of biogenic and calcareous limestone. Unit I is subdivided into four subunits: Subunit IA (0.0-50.8 mbsf; Holocene to upper Pliocene) is characterized by frequent downcore variations in carbonate content, and by a turbidite-free sedimentary sequence with only a few rare and thin volcanic ash layers. Subunit IB (50.8-370.5 mbsf; upper Pliocene - upper Miocene) is a thick interval of relatively uniform micritic biogenic ooze, with volcanic ash layers common throughout, and a few turbidites occurring in the lower half of the subunit. Subunit IC (370.5-486.0 mbsf; upper Miocene - middle Miocene) is defined by an interval of lower carbonate content, where detrital clays and quartz reach a maximum for the site. Subunit ID (486.0-513.4 mbsf; middle Miocene) is similar in lithologic characteristics to Subunit IB, though it is turbidite-free. Unit II is subdivided into two subunits: Subunit IIA (513.4-591.3 mbsf; middle Miocene - lower Miocene) is characterized by relatively high carbonate content. Subunit IIB (591.3-695.9 mbsf; lower Miocene) is characterized by fluctuating carbonate content values and the highest abundance of volcanic ash layers and turbidites of any subunit.

Sedimentation and mass accumulation rates (MARs) decline from values of 37.2 m/m.y. and 3.5–5.0 g/cm^2/k.y. in the upper Miocene to upper Pliocene interval (2.8–9.6 Ma) to an average of 27.3 m/m.y. and 2.4–3.4 g/cm^2/k.y. in the upper Pliocene-Pleistocene interval (0.0–2.8 Ma). A similar pattern was observed at Sites 998 and 999. One notable feature of the Pliocene is the abrupt increase in carbonate MARs at about 4.1–4.2 Ma, which could be the downstream expression of closing of the Central American Seaway.

Lithologic Subunits IC and ID display the highest sedimentation and accumulation rates of the section, averaging 47.0 m/m.y. and 4.5-7.5 g/cm^2/k.y., repectively. The most distinctive pattern in this part of the section is the peak in non-carbonate MARs associated with the “carbonate crash,” a trend also observed at Sites 998 and 999 (Figs. 9 and 10). At Site 1000, this interval is characterized by higher magnetic susceptibility, distinctly lower but highly variable carbonate contents, increased non-carbonate MARs, enrichments of up to 0.8% TOC (in the interval ~360–510 mbsf), and relatively high concentrations of uranium.

Sulfate reduction is more pronounced at Site 1000 compared to Sites 998 and 999, with sulfate concentrations approaching zero by 350-400 mbsf (top of the carbonate minimum and hydrocarbon enrichment zones). Paleomagnetic intensities indicate, however, that all but the upper 22.5 m of the section have been severely affected by reduction diagenesis. There are also enrichments of volatile hydrocarbons in the interval from ~400 to 520 mbsf (Fig. 12). Migration of hydrocarbons (updip and/or upsection) into the interval of the carbonate minimum (“carbonate crash”) is suspected due to the shallow burial and the absence of an anomalously high thermal gradient. No in situ generation of thermogenic gases within the “hydrocarbon zone” is supported, although bacterial methanogenesis may be a factor for the occurrence of C1 in this zone given the absence of sulfate at this depth. Increased alkalinity associated with sulfate reduction in the carbonate minimum and “hydrocarbon zone” may be responsible for the precipitation of carbonate cements along a lithification front represented by the abrupt change from chalk to limestone at about 510 mbsf (lithologic Unit I/II boundary; Fig. 12).

Many of the turbidites occurring in Subunit IIB contain redeposited pelagic sediments, but some also contain material derived from the upper reaches or tops of the adjacent carbonate banks. The lower Miocene-lower middle Miocene interval represented by the limestones and interbedded ash layers and turbidites of lithologic Unit II (13.5-20.0 Ma) had an average sedimentation rate of 27.3 m/m.y. with widely varying bulk mass accumulation rates of 3.5-6.3 g/cm^2/k.y.

The accumulation rate and number of volcanic ash layers during early to middle Miocene time at Site 1000 exhibit a pattern that is remarkably close to that of Site 999, although the magnitudes of these parameters are somewhat higher at the latter site (Fig. 4). The combined evidence from Sites 998, 999, and 1000 shows that the Miocene explosive volcanic episode generated a principal fallout axis that trends east from the Central American arc, between Sites 999 and 1000, or very close to the latitude of Site 1000. This is consistent with derivation of the tephra from the ignimbrite-forming volcanism in the Tertiary Igneous Province of Central America. The combined thickness of ash layers observed in the Caribbean sites indicates that this represents one of the major explosive volcanic episodes known. The magnitude of individual eruptive events is of the order 10^2 to 10^3 km^3, while the fallout of the episode as a whole is certainly in excess of 10^5 and probably greater than 10^6 km^3.

Site 1001

Site 1001 is located in an area of the lower Nicaraguan Rise where the Neogene sediments are thin, and where a continuous Upper Cretaceous-Paleogene sedimentary sequence overlying basaltic basement was expected. The interval between the widespread Caribbean seismic reflectors A'' (lower Eocene cherts) and B" (Upper Cretaceous basalt) had been cored but poorly recovered at DSDP Site 152, located ~40 km to the east-northeast, at the base of the Hess Escarpment. At 3270 m water depth, Site 1001 is 600 m shallower than Site 152, and is located on the Hess Escarpment. The principal objectives at Site 1001 were to (1) recover a complete Cretaceous/Tertiary boundary sequence, (2) address topics of ancient ocean paleoceanography, including the tropical record of the late Paleocene thermal maximum and the nature of orbital forcing during the Maastrichtian and Paleocene, and (3) recover igneous basement and test models of the formation of the Caribbean Oceanic Plateau. Most of the Paleogene and Cretaceous section was double-cored including the conformable basalt/limestone contact. Basalt of probable mid-Campanian age (~77 Ma) was penetrated at 485.4 mbsf, and 37.4 m of the basalt was cored.

A 165.7 m Neogene section, spanning the middle Miocene to Pleistocene, is separated from the underlying Paleogene-Cretaceous section by a pair of unconformities in Section 165-1001A-18R-4. Middle Miocene nannofossil ooze unconformably overlies middle Eocene chalk, but the middle Eocene chalk is only 28 cm thick. A second unconformable contact is marked by a chert layer where the thin middle Eocene chalk overlies lower Eocene chalk. The duration of these hiatuses is approximately 30 m.y. and 8 m.y., respectively.

Four lithologic units are recognized at this site (Fig. 13). Unit I is subdivided into four subunits: Subunit IA (6.4-112.2 mbsf; Pleistocene-upper Miocene) consists of clayey nannofossil mixed sediment to nannofossil ooze with clay. Subunit IB (112.2-131.7 mbsf; upper Miocene) is a clayey nannofossil ooze with foraminifers and is marked by a sharp increase in carbonate content and increased induration. Subunit IC (131.7-153.2 mbsf; upper Miocene-middle Miocene) is composed of nannofossil ooze with clay to nannofossil clay and is distinguished from the intervals above and below by the highly variable carbonate contents and magnetic susceptibility. Subunit ID (153.2-165.7 mbsf; middle Miocene) contains nannofossil ooze with clay to clayey nannofossil ooze; this interval is distinctly more carbonate-rich than Subunit IC and has much lower and less variable values of magnetic susceptibility.

Lithologic Unit II corresponds with the Paleocene-Eocene section. The distribution of chert is the principal feature used to subdivide Unit II into two subunits. Subunit IIA (165.7-304.6 mbsf; middle and lower Eocene-upper Paleocene) is primarily composed of calcareous chalk with foraminifers to mixed sedimentary rock with clay. This subunit is interbedded with numerous chert and volcanic ash layers. Subunit IIB (304.6-352.1 mbsf; upper Paleocene-lower Paleocene) lacks the cherts of Subunit IIA. It is more clay-rich, especially in the lower Paleocene, and is further distinguished by the presence of thin interbedded foraminiferal-rich sand layers. The dominant lithologies of Subunit IIB are calcareous chalk with clay to claystone and some ash layers.

The Cretaceous/Tertiary boundary interval was recovered in both Hole 1001A and Hole 1001B (Sections 165-1001A-38R-CC and 39R-1, and Section 165-1001B-18R-5). Comparison of the Formation MicroScanner (FMS) data and the recovered sediments indicates that 15-20 cm of the boundary deposit may not have been recovered (Fig. 14). Remarkably, however, several clay-rich units between the basal Paleocene and upper Maastrichtian limestones were recovered. A 1.7-4.0 cm light gray, highly indurated limestone of earliest Paleocene age (planktonic foraminifer Zone P0/Pa, undifferentiated), similar to the limestone recovered earlier at Site 999, overlies the package of clay-rich strata constituting the bulk of the recovered boundary deposit at Site 1001. The topmost layer of the boundary deposit is a 3.5-cm-thick, massive clay. This unit contains rare grains of shocked quartz and overlies a 3.5-cm-thick smectitic claystone with dark green spherules. The spherules are up to 2 mm in diameter, and may represent altered tektites from the K/T impact event. The base of the boundary deposit is a 1-to 2-cm-thick smectitic clay layer with shaley cleavage. This clay contains light-colored speckles, up to 1 mm in diameter. In addition to these three distinctive clay layers, two loose pieces of polymict micro-breccia were recovered from the top of Core 165-1001A-39R. These contain angular clasts (<6 mm) of claystone and limestone in an unconsolidated matrix of smectitic clay. This lithology may represent fragments of a thicker poorly recovered unit at this site. The total boundary deposit has an inferred thickness of approximately 25 cm at this location.

The Upper Cretaceous sedimentary section is represented by lithologic Unit III, which is subdivided into two subunits. A marked increase in carbonate content delimits the change from lower Paleocene mixed sedimentary rocks and claystones to Maastrichtian limestone. Subunit IIIA (352.1-472.9 mbsf; basal Paleocene to mid-Campanian) consists of calcareous limestone and claystone with interbedded foraminiferal-rich sand layers. Ash layers become thicker and more frequent in the lower part of Subunit IIIA. Subunit IIIB (472.9-485.4 mbsf; mid-Campanian) is characterized by a significant reduction in carbonate content and a dramatic increase in the abundance of altered volcaniclastic material, including common andesitic to silicic ash fall layers and several thick ash turbidites. The lower part of this unit contains angular to subangular fragments of basaltic lapilli and hyaloclastite breccia that grade downcore into a conformable basement contact consisting of sediment-poor basaltic lapilli and basalt.

Lithologic Unit IV (485.4-522.8 mbsf; mid-Campanian), the igneous basement, consists of a succession of 12 formations, which likely represent individual pillow lavas and sheet flows. Some of the flows have thick hyaloclastite breccia tops and massive columnar interiors.

Several lines of evidence support the hypothesis that the volcanic edifice cored at Site 1001 subsided rapidly in mid-Campanian time. Vesicles in the basalt are relatively large, suggesting water depths significantly shallower than the present. Benthic foraminifers from limestone lenses between the basalt flows suggest neritic paleodepths, whereas a rapidly deepening upward trend is suggested on the basis of benthic foraminifer assemblages in the overlying limestones and ash turbidites. The volcanic edifice was likely located near the paleoequator as suggested by the very shallow paleomagnetic inclinations obtained from the basalt and overlying sediments.

A carbonate-poor, clay-rich interval in the uppermost Paleocene is similar to a correlative interval cored earlier at Site 999. Both sites contain volcanic ash layers within the distinctive laminated to weakly bioturbated deposit. We attribute the character of this interval to the rapid and short-lived oceanographic changes of the “late Paleocene thermal maximum.” The interval was cored and recovered twice at Site 1001 (Sections 165-1001A-27R-2 and 165-1001B-6R-3).

Ash layers representing three episodes of volcanism in the Caribbean were found in the Paleogene-Upper Cretaceous of Site 1001 (Fig. 4). One episode in the latest Paleocene-early Eocene time is likely related to the explosive volcanism documented at Site 998 and attributed to the Cayman Ridge arc. A second smaller peak of volcanism occurred in the early Paleocene, and it is perhaps contemporaneous with the activity recorded at Site 999 on the Kogi Rise and attributed to the Central American arc. A third short-lived episode occurred in mid-Campanian time, perhaps associated with the activity of central volcanoes on the Caribbean Oceanic Plateau.

The middle/upper Miocene boundary interval at Site 1001 is distinguished by highly variable carbonate contents and magnetic susceptibility, and correlates with the “carbonate crash” interval recognized at Sites 998, 999, and 1000. However, in contrast with these earlier sites, the interval of reduced carbonate values persists about one million years longer at Site 1001.

Site 1002

Site 1002 is located adjacent to DSDP Site 147 in the Cariaco Basin, a structural depression on the northern continental shelf of Venezuela that is the second largest anoxic marine body in the world, after the Black Sea. High sedimentation rates (300 to >1000 m/m.y.) and its location in a climatically sensitive region of the tropical ocean made the Cariaco Basin a prime drilling target for high-resolution studies of geologically recent climate change. The major objectives at Site 1002 were to recover a continuous and undisturbed late Quaternary stratigraphic section that will be used to (1) document how climate change in the southern Caribbean and northern South America relates to climatic forcing mechanisms and to global-scale change, especially to high latitude changes recorded in ice cores and high-deposition-rate marine sediment sequences, (2) study the rates and magnitudes of tropical climate change at interannual to millennial time scales over the last several glacial-interglacial cycles, (3) examine the stability of tropical climate in response to past changes in large-scale global boundary conditions, and (4) study the relationships between climate variability and processes that influence the burial of organic carbon in anoxic settings.

Five holes were drilled at Site 1002, two of which were mudline cores taken for geochemical studies; three more were taken for high-resolution paleoclimatic reconstructions. Only the cores from Hole 1002C were split open on board ship for preliminary descriptions and analysis. Time was short for inspection and discussion and only the most preliminary observations can be made at this time.

Hole 1002C recovered a total of 170.1 m of mostly mixed, or hemipelagic sediments. The presence of *Emiliania huxleyi* at the base of the sequence suggests that all of the sediments fall within Zone CN15, or were deposited in the past 248,000 years. This single biostratigraphic estimate is consistent with estimates based on extrapolating known sedimentation rates for the Holocene and last glacial back the length of the drilled sequence.

Sediments in Hole 1002C are generally dominated by terrigenous components with variable biogenic contributions of nannofossils, diatoms, and foraminifers. Much of the sediment is laminated, indicating deposition under largely anoxic conditions.

The sedimentary sequence at Site 1002 was assigned to one formal lithostratigraphic unit and eight subunits. Despite this degree of subdivision, there appear to be only about three major lithologies, which alternate in a semi-predictable fashion. The bulk of the sequence consists of clayey nannofossil mixed sediments, olive gray to greenish gray in color, which appear to have been deposited under both anoxic (laminated) and oxic (massive) conditions. These sediments are punctuated periodically by episodes of bluish gray and yellowish brown clay deposition, laid down under clearly oxic conditions. Generally following this, deposition of diatom-rich, distinctly laminated sediment indicates strong upwelling, such as was experienced during the early Holocene in Subunit Ib. Earlier periods of clay deposition, followed by accumulation of diatom-rich sediments, may similarly signal earlier periods of deglaciation.

SUMMARY

The cores recovered at five sites in the Caribbean Sea during Leg 165 address a number of geologic problems of great diversity. The recovery of the Cretaceous/Tertiary boundary in three holes on this leg has provided valuable new samples of the boundary deposit for the study of impact ejecta, and will help clarify the sedimentation and dispersal processes associated with the impact, and its environmental effects. The shipboard identification of shocked quartz crystals, with characteristic planar deformation features, in the uppermost claystone unit of the boundary deposit and the recovery of a smectite layer consisting of altered impact glass spherules or tektites are important contributions to the study of this catastrophic event. The use of the Formation MicroScanner logging tool was invaluable in imaging and measuring the thickness of the Cretaceous/Tertiary boundary deposit in situ, and thus evaluating the degree of recovery of the soft boundary units in each hole (Figs. 8 and 14).

The discovery of a large number of volcanic ash layers in the Caribbean sediments at four of the principal sites has established that major volcanic episodes occurred in Central America. They include particularly vigorous volcanic episodes during middle to late Eocene and early to middle Miocene times, with eruption frequency on the order of 40 events/m.y. (Fig. 4). The evidence from the petrographic and sedimentologic character of the silicic volcanic ash layers indicates that their source lies in the great rhyolitic ignimbrite eruptions on the Chortis Block in the Central American arc, more than 1000 km to the west (Fig. 15a). These great explosive events have resulted in accumulation rates of megascopic volcanic ash layers up to 250 cm/m.y. in the Caribbean. In addition, geochemical studies show that the deposition of a dispersed ash component constitutes 10% to 20% of the total sedimentary record (Fig. 5). These two episodes of large-scale vulcanism precede major high-latitude cooling steps in the Eocene and Miocene, suggesting that vulcanism may have provided important climatic feedbacks in the past. Geochemical studies of pore waters and sediments have shown that the alteration of volcanic ash components may have had a profound effect on the levels of oceanic Si and that this process may ultimately have contributed to the accumulation of the vast amount of chert that abounds in the Eocene marine record. Similarly, the altered ash layers have also served as sinks for S and Ni, in response to the weathering of the volcanic glass to tri-octahedral smectite.

Early to middle Eocene ash layers at Site 998 on the Cayman Rise, consisting of ash falls and volcaniclastic turbidites, show evidence of being derived from local sources, which implicates the Cayman Ridge (Fig. 15b). This evidence suggests that volcanic activity occurred on the Cayman arc in response to subduction, possibly from the southwest (Fig. 16). Thus, the Yucatan Basin may have opened as a backarc basin behind the Cayman volcanic arc (Fig. 15b). These findings are likely to have important implications for models of Caribbean plate tectonic evolution.

The recovery of the basalt/sediment contact in two holes at Site 1001 on the Hess Escarpment and recovery of a succession of 12 submarine lava flows of mid-Campanian age give new insights into the evolution of the later stages of the Caribbean Oceanic Plateau. The assemblage of benthic microfossils in the Campanian sediments resting on the basaltic lava flow succession, and in limestone lenses within the lavas, together with the vesicularity of the basalts, indicates rapid subsidence of the plateau in late Campanian time. Submarine lavas in this succession are of two principal types: massive sheet flows attributed to high mass eruption rates, and pillow lavas. The results show that Caribbean Oceanic Plateau volcanism continued at least until 77 Ma, and activity of central volcanoes on the plateau may have persisted until 74 Ma. These findings are therefore in disagreement with models that propose extremely rapid outpouring of the plateau in the 88-90 Ma time frame.

A transient episode of rapid warming during latest Paleocene time occurred within a longer-term interval of increasing temperatures that culminated in the early Eocene (Zachos et al., 1993). This was a time of abrupt change from the tropics to the poles. In the southern high latitudes, sea surface temperatures increased from 14° to 20°C in less than 10,000 years while deep water temperatures warmed from 10°C to 18°C (Stott and Legan, 1990; Kennett and Stott, 1991). This episode of extreme high-latitude warmth lasted for up to several hundred thousand years (Zachos et al., 1993). The “late Paleocene thermal maximum” is also marked by a large negative $\delta^{13}C$ excursion and a mass extinction in deep water benthic foraminifers (Thomas, 1990, 1992; Kennett and Stott, 1991). In the tropics, thermal gradients between the surface and intermediate waters collapsed and benthic foraminifers record a 4°-6°C warming of intermediate waters coeval with the $\delta^{13}C$ excursion and benthic foraminiferal extinction (Bralower et al., 1995). Extreme oligotrophy in the equatorial Pacific stimulated a burst of diversification among the surface-dwelling, photosymbiont-bearing planktonic foraminiferal genera *Acarinina* and *Morozovella* (Kelly et al., 1996). A rapid but short-lived change from high-latitude to low-latitude sources of deep (and intermediate?) water masses is suspected to be responsible for the extreme warming event (Kennett and Stott, 1991; Pak and Miller, 1992).

Uppermost Paleocene sequences recovered during Leg 165 record the effect of the late Paleocene thermal maximum (LPTM) on the surface and deep waters of the Caribbean. Sites 999 and 1001 (Holes 1001A and 1001B) provide a unique record of the LPTM; for the first time the event can be observed from lithologic and physical property changes and on downhole logging measurement. In both sites, this interval corresponds to a claystone unit, up to a meter thick, characterized by significantly lower carbonate contents than surrounding chalks and limestones. This claystone shows faint lamination in places and indications of diminished bioturbation in others, the strongest evidence of reduced seafloor oxygenation in any LPTM record. Pronounced maxima are seen on gamma ray and susceptibility records. Interbedded in the claystone are three multicolored volcanic ash horizons, which allow precise correlation between the sections at Site 999 and 1001, and between the two holes in the latter site.

Because the paleodepths of Sites 999 and 1001 are deeper than most other LPTM sections, these records add important constraints to our knowledge of deep water circulation and chemistry during the event. Diminished carbonate contents in claystones are thought to reflect shoaling of the lysocline and CCD in the LPTM interval, among the first evidence for changes in the corrosiveness of deep waters at this time. Evidence for dysoxia suggests that only the deepest part of the water column was truly oxygen-deficient, that the Caribbean deep waters were very old, or alternatively, that a source of warm, saline deep waters was close by. Alternatively, reduced carbonate flux, rather than dissolution, may be the principal reason for the reduced carbonate content. This is supported by the lack of measurable organic carbon in the claystone at either site, and is compatible with other lines of evidence for surface water oligotrophy during the LPTM interval (Rea et al., 1990; Kelly et al., 1996). The late Paleocene-early Eocene records at these sites also reveal episodic winnowing of sediments, indicating active bottom-water circulation during a time of global warmth.

Another important discovery of Leg 165 is a marked reduction in pelagic carbonate deposition near the middle/late Miocene boundary interval about 10.5-12.5 Ma at Sites 998, 999, 1000, and 1001 (Figs. 6 and 10). A similar regional event is well-known from the central and eastern equatorial Pacific (e.g., van Andel et al., 1975; Farrell et al., 1995) and is referred to as the “carbonate crash” by Lyle et al. (1995). This event had not been previously documented in the Caribbean Sea. Drilling during Leg 165 revealed that the “carbonate crash” occurred widely across the Caribbean including the Colombian Basin (Sites 999 and 1001), on the Cayman Rise (Site 998) and, to a lesser degree, on northern Nicaragua Rise in Pedro Channel (Site 1000). At Site 1000, the sea bottom (912 m) is at the base of the permanent thermocline. The carbonate records in the equatorial Atlantic Ocean (Ceara Rise, Leg 154; Curry, Shackleton, Richter, et al., 1995) show also that carbonate values decrease dramatically during the same time interval.

A major fall in global sea level at ~10.5-11.0 Ma (Haq et al., 1987) appears to be synchronous with the end of the “carbonate crash” in the Caribbean, and could explain the high accumulation rates of noncarbonate components at that time (Fig. 9). This increase of noncarbonate input into the ocean due to exposure of continental shelves would have enhanced the dilution effect of the “carbonate crash.” Preliminary results of Leg 165 seem to show that the initiation of the carbonate crash and its nadir (between 12.5 and 10.5 Ma) in the Caribbean are synchronous with observations from the eastern, central, and western equatorial Pacific, as well as from the equatorial Atlantic. The carbonate crash in the eastern equatorial Pacific seems to have lasted for another 1.0 to 1.5 Ma. The results from Leg 165 add important constraints as to the timing and geographic extent of the “carbonate crash.” Post-cruise study will investigate the link between this event and the formation of Miocene gateways and sills, changes in oceanic circulation, and variations in water-mass sources and chemistry.

The final closing of the Central American Seaway during the Pliocene also had a profound influence on:

- shifting loci of tropical productivity;
- the evolution of the salt imbalance between the Caribbean and the eastern Pacific, and;
- the global ocean conveyor and on the evolution of the endemic Atlantic microbiota.

The anoxic Cariaco Basin on the margin of Venezuela has yielded a triple-cored record (Site 1002) of latest Quaternary tropical climate variability that can be studied on time scales of tens to hundreds of years. This record also will permit studies of links in tropical-polar climate change back 200,000 yr.

References

Bralower, T.J., Zachos, J.C., Thomas, E., Parrow, M., Paull, C.K., Kelly, D.C., Premoli Silva, I., Sliter, W.V., and Lohmann, K.C., 1995. Late Paleocene to Eocene paleoceanography of the equatorial Pacific Ocean: stable isotopes recorded at Ocean Drilling Program Site 865, Allison Guyot. *Paleoceanography,* 10:841-865.

Curry, W.B., Shackleton, N.J., Richter, C., et al., 1995. *Proc. ODP, Init. Repts*., 154: College Station, TX (Ocean Drilling Program).

Droxler, A.W., Cunningham, A., Hine, A.C., Hallock, P., Duncan, D., Rosencrantz, E., Buffler, R., and Robinson, E., 1992. Late middle(?) Miocene segmentation of an Eocene-early Miocene carbonate megabank on the northern Nicaragua Rise: *Eos, Suppl*., 73, S299.

Farrell, J.W., Raffi, I., Janecek, T.R., Murray, D.W., Levitan, M., Dadey, K.A., Emeis, K-C., Lyle, M., Flores, J-A., and Hovan, S., 1995. Late Neogene sedimentation patterns in the easter equatorial Pacific Ocean. *In* Pisias, N.G., Mayer, L.A., Janecek, T. R., Palmer-Julson, A., and van Andel, T.H. (Eds.), *Proc. ODP, Sci. Results,* 138: College Station, TX (Ocean Drilling Program), 717-756.

Haq, B.U., Hardenbol, J., and Vail, P.R., 1987. Chronology of fluctuating sea levels since the Triassic. *Science*, 235:1156-1167.

Kelly, D.C., Bralower, T.J., Zachos, J.C., Premoli Silva, I., and Thomas, E., 1996. Rapid diversification of planktonic foraminifera in the tropical Pacific (ODP Site 865) during the late Paleocene thermal maximum. *Geology.*

Kennett, J.P., and Stott, L.D., 1991. Abrupt deep-sea warming, palaeoceanographic changes and benthic extinctions at the end of the Palaeocene. *Nature*, 353:225-229.

Lyle, M., Dadey, K.A., and Farrell, J.W., 1995. The late Miocene (11-8 Ma) eastern Pacific carbonate crash: evidence for reorganization of deep-water circulation by the closure of the Panama Gateway. *In* Pisias, N.G., Mayer, L.A., Janecek, T. R., Palmer-Julson, A., and van Andel, T.H. (Eds.), *Proc. ODP, Sci. Results*, 138: College Station, TX (Ocean Drilling Program), 821- 838.

Pak, D.K., and Miller, K.G., 1992. Paleocene to Eocene benthic foraminiferal isotopes and assemblages: implications for deepwater circulation. *Paleoceanography*, 7:405-422

Perfit, M.R., and Heezen, B.C, 1978. The geology and evolution of the Cayman Trench. *Geol. Soc. Am. Bull.*, 89:1155-1174.

Pindell, J.L., and Bartlett, S.F., 1990. Geological evolution of the Caribbean region; a plate-tectonic perspective. *In* Dengo, G., and Case, J.E. (Eds.), *The Geology of North America*, Geol. Soc. Amer., H:405-432.

Rea, D.K., Zachos, J.C., Owen, R.M., and Gingerich, P.D., 1990. Global change at the Paleocene-Eocene boundary: climatic and evolutionary consequences of tectonic events. *Palaeogeogr., Palaeoclimatol., Palaeoecol.*, 79:117-128

Rosencrantz, E., and Sclater, J.G., 1986. Depth and age in the Cayman Trough. *Earth Planet. Sci. Lett.*, 79:133-144.

Scott, D.B., and Leger, G.T., 1990. Benthic foraminifers and implications for intraplate deformation, Site 717, distal Bengal Fan. *In* Cochran, J.R., Stow, D.A.V., et al., *Proc.ODP, Sci. Results*, 116: College Station, TX (Ocean Drilling Program), 189-206.

Thomas, E., 1990. Late Cretaceous through Neogene deep-sea benthic foraminifers (Maud Rise, Weddell Sea, Antarctica). *In* Barker, P.F., Kennett, J.P., et al., *Proc. ODP, Sci. Results*, 113: College Station, TX (Ocean Drilling Program), 571-594.

Thomas, E., 1992. Cenozoic deep-sea circulation: evidence from deep-sea foraminifers. *In* Kennett, J.P., and Warnke, D.A. (Eds.), *The Antarctic Paleoenvironment: A Perspective on Global Change*. Am. Geophys. Union, Antarctic Res. Ser., 56:141-165.

van Andel, T.H., Heath, G.R., and Moore, T.C., 1975. Cenozoic tectonics, sedimentation, and paleoceanography of the central equatorial Pacific. *Geol. Soc. Amer.,* Mem., 143.

Zachos, J.C., Lohmann, K.C., Walker, J.C.G., and Wise, S.W., 1993. Abrupt climate change and transient climates during the Paleogene: a marine perspective. *J. Geology*, 101:191-213.

FIGURE CAPTIONS

Figure 1. A map of the Caribbean Sea, showing the location of ODP Leg 165 sites and sites drilled during DSDP Leg 15.

Figure 2. Summary of correlations between seismic stratigraphy, depths, logging units, lithologic units, and ages at Site 998. Velocities shown are averages derived from the sonic velocity tool within each logging unit. The 1.65 km/s velocity is an average of 1.5 km/s at the seafloor and the first log velocity of 1.8 km/s at 180 mbsf. Although total depth at Hole 998B is 904.8 mbsf, Logging Unit 5 is only defined to 880 mbsf. The bottom of Hole 998B at 904.8 mbsf corresponds to 5 s twt, and volcanic basement lies at 5.15 s twt.

Figure 3. Turbidite frequency and the median and total bed thicknesses vs. age at Site 998.

Figure 4. The distribution of volcanic ash layers at four sites drilled during Leg 165, Site 999 on the Kogi Rise in the Colombian Basin, Site 998 on the Cayman Rise, Site 1000 on the upper Nicaraguan Rise, and Site 1001 on the Hess Escarpment. The figure shows the accumulation rate of megascopic volcanic ash layers as cm/m.y. The data are not corrected for core recovery, as, in general, core recovery was excellent and close to complete in much of the cored section. The distribution of volcanic ash layers defines five volcanic episodes: (1) early to mid-Miocene, (2) mid- to late Eocene, (3) late Paleocene to earliest Eocene, (4) early Paleocene, and (5) late Campanian.

Figure 5. The dispersed ash and terrigenous component in sediments drilled during Leg 165 calculated on the basis of geochemical normative models.

Figure 6. Correlation between %CaCO3 and magnetic susceptibility data for pelagic carbonates at Site 998 and comparison with the Miocene “carbonate crash” equatorial Atlantic (Leg 154) and Pacific (Leg 138) sites from prior ODP legs.

Figure 7. Summary of correlations between seismic stratigraphy, depths, logging units, lithologic units, and ages at Site 999. The location of Site 999 marked on this profile is 800 m west of the actual site location determined by GPS. Correlations with the reflection seismic record were constrained by calculations of two-way traveltime vs. depth derived from compressional velocities measured by downhole logging and laboratory instruments. Velocities shown are averages derived from the downhole sonic tool within each major logging unit. The total depth at Hole 999B of 1066.4 mbsf corresponds to 4.722 twt. The depth of volcanic basement is approximately 1400 mbsf if average velocities measured within seismic unit CB5 are extended to 4.936 s twt.

Figure 8. An overview of the Cretaceous/Tertiary boundary at Site 999. At left is a lithostratigraphic summary of the boundary. The second column from the left shows a photograph of the core sections including and adjacent to the boundary (Sections 165-999B-59R-3, 59R-CC, and 60R-1). In the right center is an image of the boundary

from the Formation MicroScanner log (FMS) of the hole. In this image the limestone above the boundary appears light gray (a low conductivity layer), whereas the claystone above and below the boundary is dark (high conductivity layers). The FMS image shows a claystone layer at the base of the limestone, which is about 8 cm thicker than the recovered claystone deposit. We propose that this represents the portion of the boundary deposit that was not recovered. On the far right is magnetic susceptibility log of the recovered core.

Figure 9. Mass accumulation rates for the carbonate and non-carbonate components for the interval bounding the middle/late Miocene “carbonate crash” at Sites 998, 999 and 1000.

Figure 10. Correlation between %CaCO3 and magnetic susceptibility data for pelagic carbonates at Sites 998, 999, and 1000.

Figure 11. Summary of correlations between seismic stratigraphy, depths, logging units, lithologic units, and ages at Site 1000. Correlations with the reflection seismic record were constrained by calculations of two-way traveltime versus depth derived from compressional velocities measured by downhole logging and laboratory instruments. Velocities shown are averages derived from the downhole sonic tool within each major logging unit.

Figure 12. Alkalinity in Site 1000 interstitial waters compared to bulk calcium carbonate contents of sediment. Arrow indicates mean ocean bottom water sulfate composition.

Figure 13. Summary of correlations between seismic stratigraphy, depths, logging units, lithologic units, and ages at Site 1001. Velocities above basement are interval velocities derived from two-way traveltimes to the two prominent reflections A” and B” and from drilling depths to each of these seismic horizons. In lithologic Unit IV (volcanic basement) the average velocity from laboratory measurements is given (4.672 km/s) and is used to calculate total depth at 4.736 s twt. An approximately 2-km portion of EW9417 SCS line 10 is displayed with a vertical exaggeration of 10x.

Figure 14. The Cretaceous/Tertiary boundary at Site 1001 on the lower Nicaraguan Rise. On the left is a lithostratigraphy description of the recovered boundary deposit in Section 165-1001B-18R-5. In the center is a core photograph of the unsplit Section 165-1001B-18R-5, (15-55 cm). Note that the dark specks on the surface of the upper Maastrichtian limestone are smectite particles that have been eroded from the basal part of the boundary deposit during drilling. On the right is the Formation MicroScanner downhole log of the K/T boundary interval. The FMS record shows a high-resistivity band (bright to white), which we interpret to reflect the hard limestone immediately above the K/T boundary. It is underlain by a 30-cm-wide zone of low to very low (dark) resistivity, which we interpret as the K/T boundary deposit. The interpretation of downhole magnetic susceptibility logging data of Hole 1001A (See “Physical Properties” section, chapter 1001) and comparison with the magnetic susceptibility log of the recovered cores are also consistent with a 20-to-30

cm-thick in situ boundary deposit at this site. Thus approximately only a third of the deposit was recovered by drilling.

Figure 15. Drilling during Leg 165 recovered volcanic ash layers in Caribbean sediments that have originated by two modes of deposition. Silicic ash layers in the Colombian Basin (A; Sites 999 and 1001) and on the Nicaraguan Rise (Site 1000) are dominantly derived as co-ignimbrite ash fallout from major ignimbrite-forming explosive eruptions in the Central American arc to the west. They are deposited from eruption plumes that are transported to the east in the lower stratosphere. In contrast, many of the Eocene ash layers recovered on the Cayman Rise (B; Site 998) are volcaniclastic turbidites, derived from a relatively local source. We propose that they owe their origin to Eocene activity of the Cayman volcanic arc to the south.

Figure 16. The plate tectonic setting of the Cayman Ridge volcanic arc and the Cayman Rise in the Eocene, based on the results of Site 998 drilling, and from dredging in the Cayman Trough (Perfit and Heezen, 1978). Relations in southeastern Cuba and north Hispaniola are based on Pindell and Bartlett (1990). The Cayman arc is attributed to a northerly subduction of the leading edge of the Caribbean Plate, after collision of the Cuban arc with the Bahamas platform has choked off subduction beneath the Cuban arc. The Eocene (and Paleocene?) subduction beneath the Cayman arc may also have led to backarc rifting of the Yucatan Basin. The middle Eocene cessation of Cayman arc volcanism is taken as the timing of choking of the Cayman arc trench by the thicker component of the Caribbean Plate, leading to a change in the North American-Caribbean plate boundary from one of subduction to one of strike-slip, with the initiation of the Cayman Trough in the middle to late Eocene (Rosencrantz and Sclater, 1986).

Figure 1.

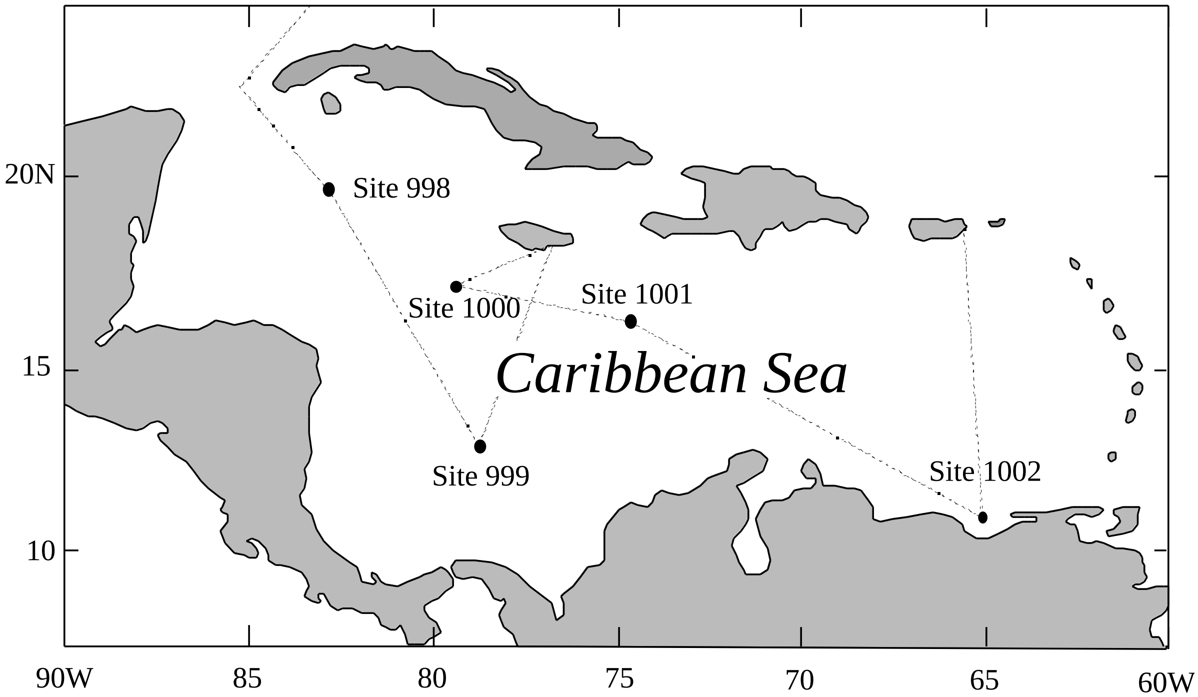
20N
15
10
90W
85
80
75
70
65
60W
Site 998
Site 1000
Site 1001
Caribbean Sea
Site 999
Site 1002

Figure 2.

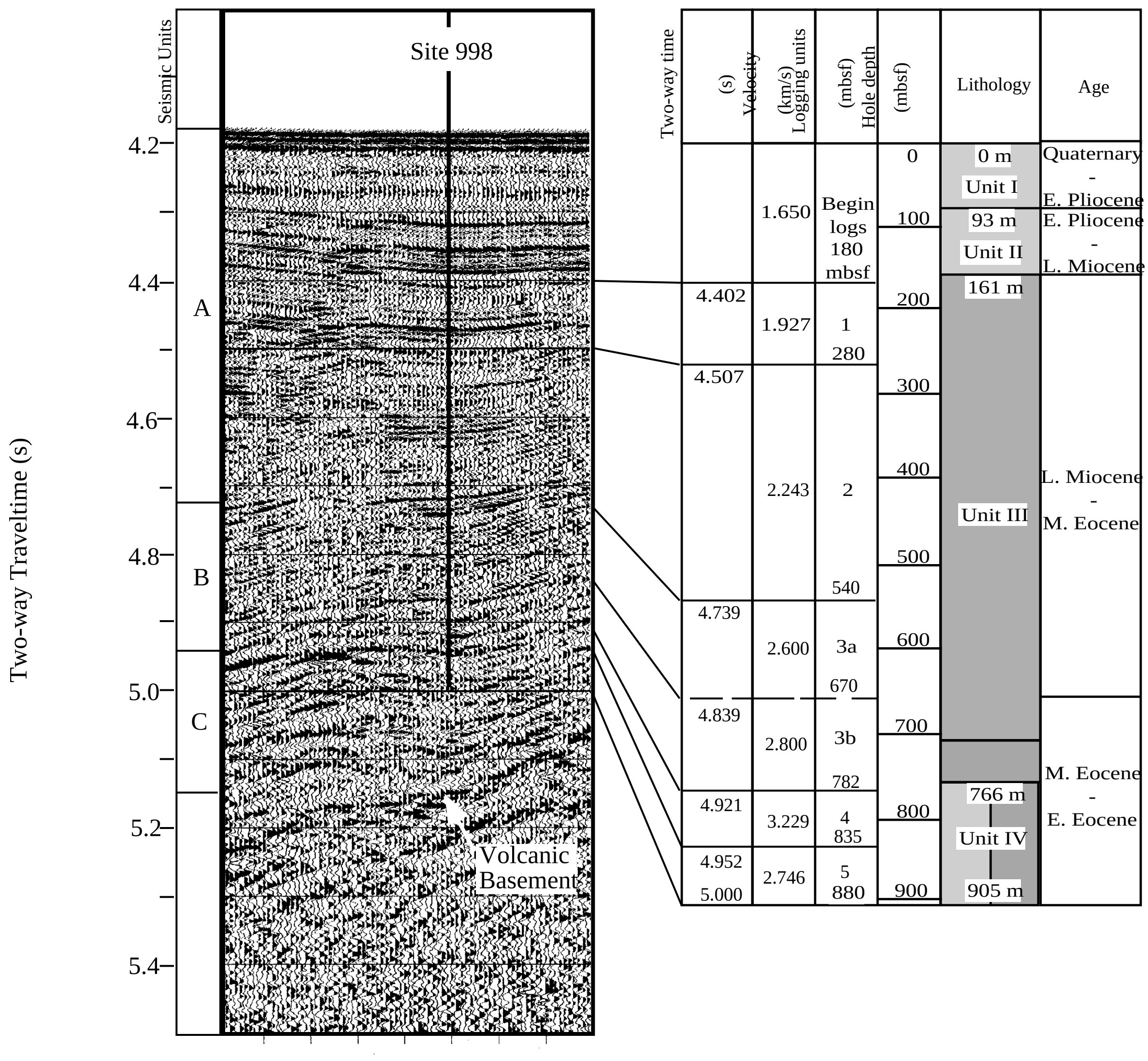
Seismic Units
Site 998
Two-way Traveltime (s)
4.2
4.4
4.6
4.8
5.0
5.2
5.4
A
B
C
Volcanic Basement
Two-way time (s)
Velocity (km/s)
Logging units
Hole depth (mbsf)
(mbsf)
Lithology
Age
4.402
4.507
4.739
4.839
4.921
4.952
5.000
1.650
1.927
2.243
2.600
2.800
3.229
2.746
Begin logs 180 mbsf
1
280
2
540
3a
670
3b
782
4
835
5
880
0
100
200
300
400
500
600
700
800
900
0 m
Unit I
93 m
Unit II
161 m
Unit III
766 m
Unit IV
905 m
Quaternary - E. Pliocene
E. Pliocene - L. Miocene
L. Miocene - M. Eocene
M. Eocene - E. Eocene

Figure 3.

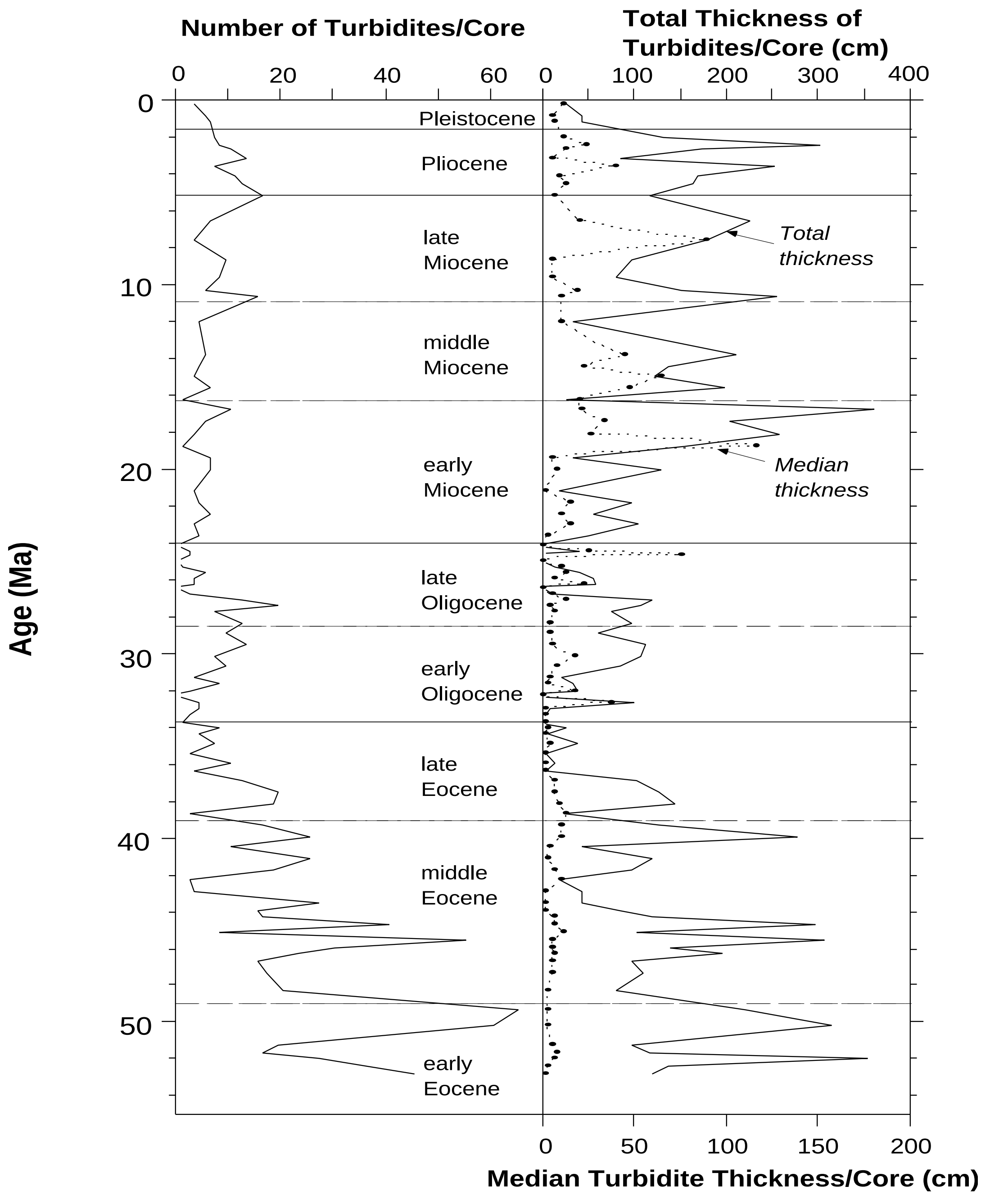
Number of Turbidites/Core
Total Thickness of Turbidites/Core (cm)
0
20
40
60
0
100
200
300
400
Age (Ma)
0
10
20
30
40
50
Pleistocene
Pliocene
late Miocene
middle Miocene
early Miocene
late Oligocene
early Oligocene
late Eocene
middle Eocene
early Eocene
Total thickness
Median thickness
0
50
100
150
200
Median Turbidite Thickness/Core (cm)

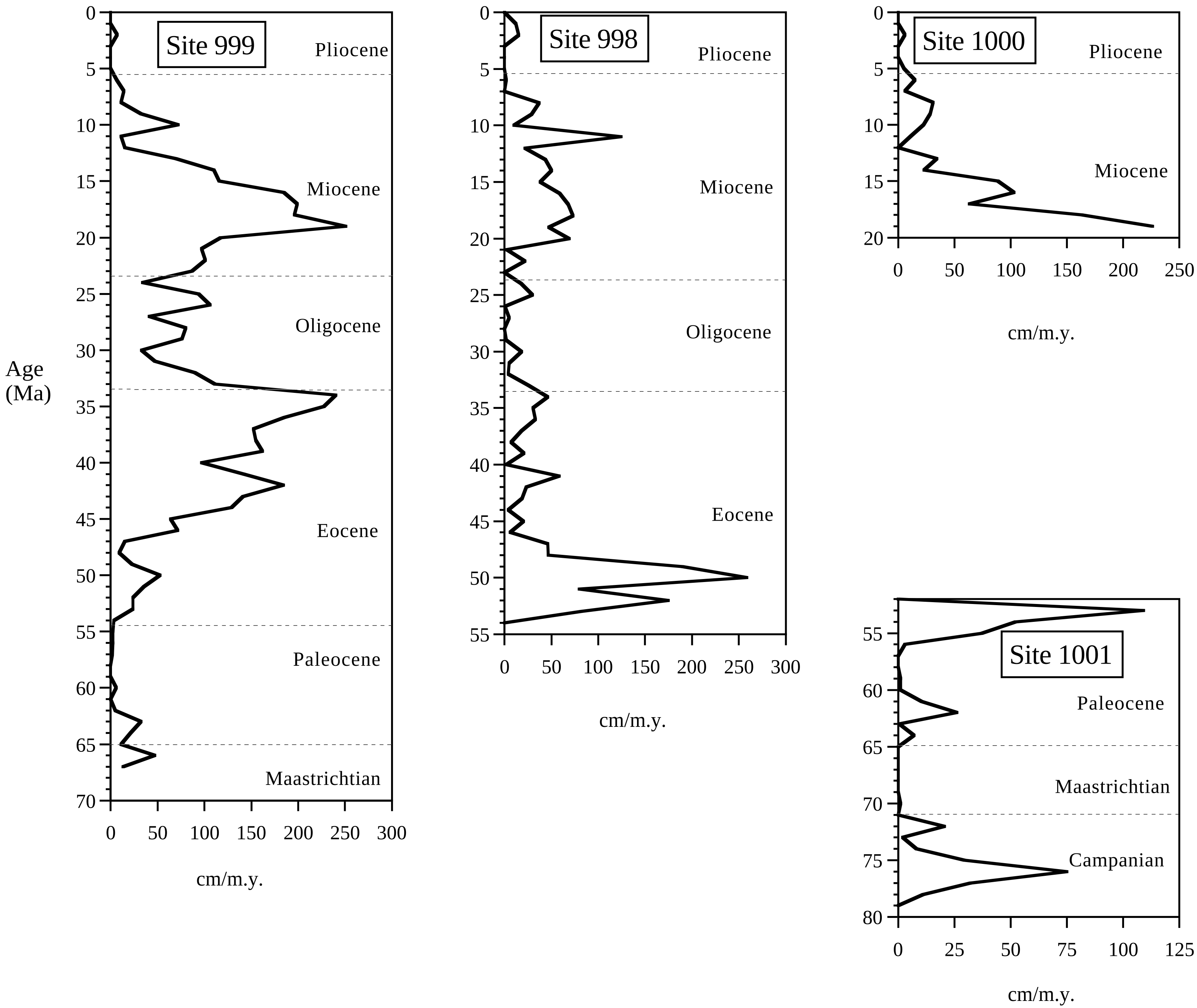
Site 999
Site 998
Site 1000
Site 1001
Age
(Ma)
Pliocene
Miocene
Oligocene
Eocene
Paleocene
Maastrichtian
Campanian
cm/m.y.
0
5
10
15
20
25
30
35
40
45
50
55
60
65
70
75
80
100
125
150
200
250
300

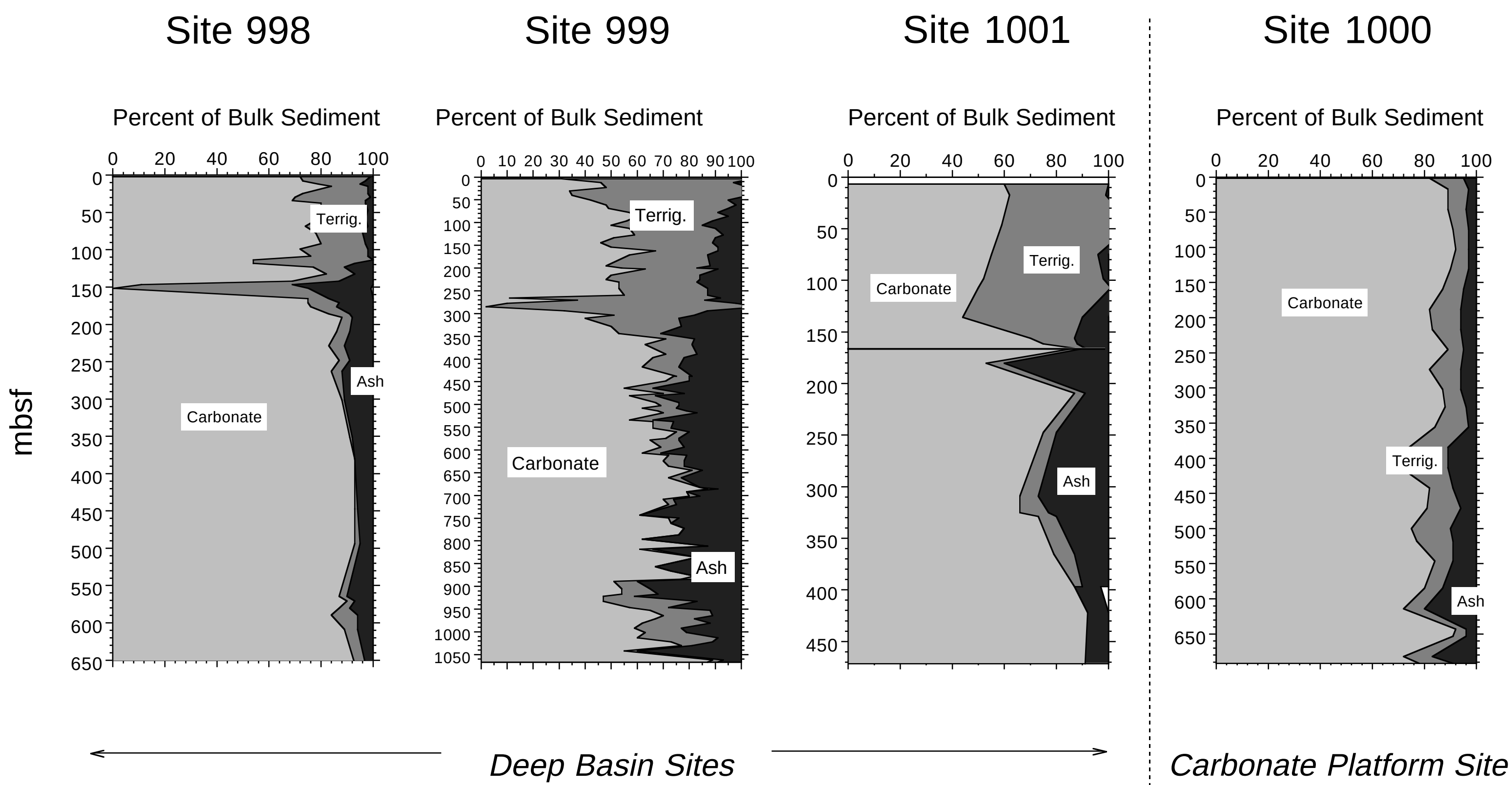

Site 998
Site 999
Site 1001
Site 1000
Percent of Bulk Sediment
Percent of Bulk Sediment
Percent of Bulk Sediment
Percent of Bulk Sediment
mbsf
Terrig.
Ash
Carbonate
Deep Basin Sites
Carbonate Platform Site

Fig. 165-13

Figure 6.

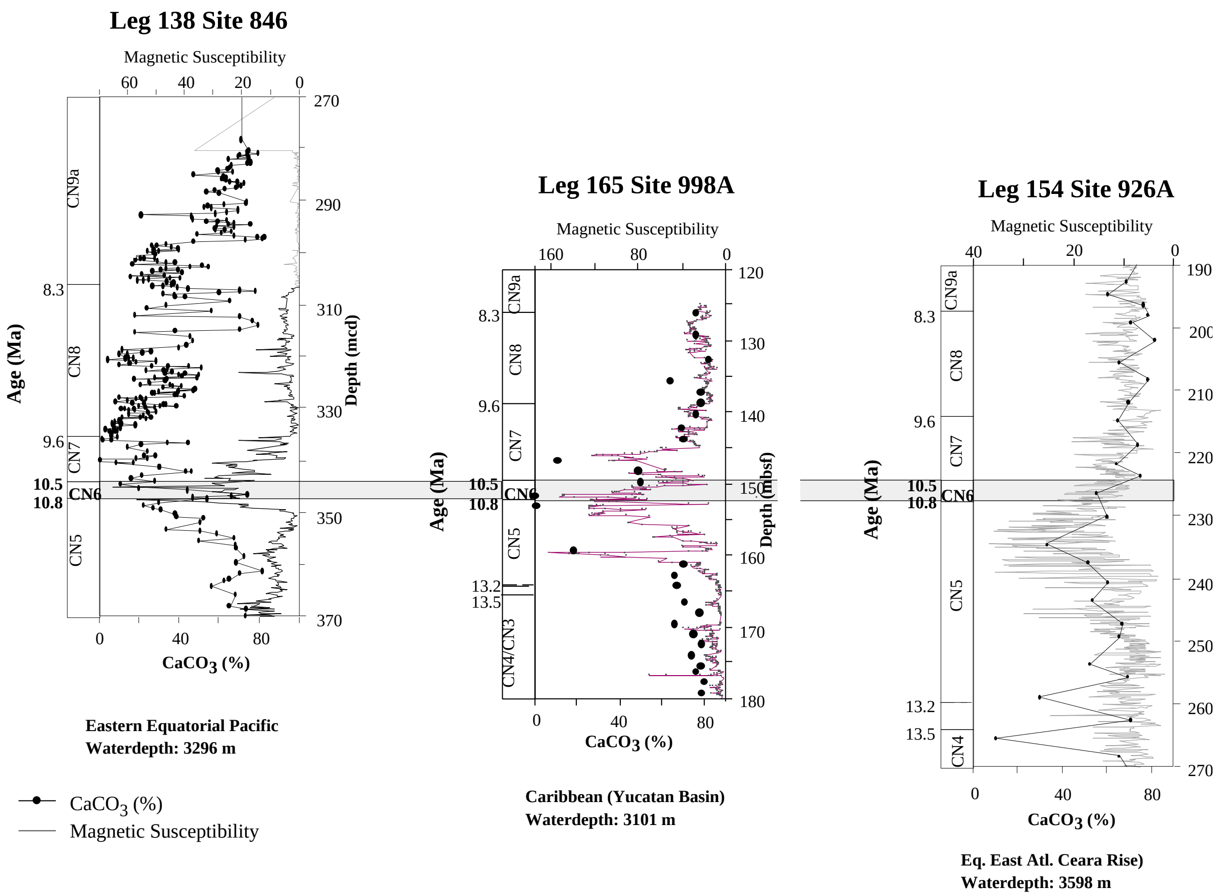
Leg 138 Site 846
Magnetic Susceptibility
60 40 20 0
270
290
310
330
350
370
Depth (mcd)
Age (Ma)
CN9a
8.3
CN8
9.6
CN7
10.5
CN6
10.8
CN5
0 40 80
CaCO3 (%)
Eastern Equatorial Pacific
Waterdepth: 3296 m
CaCO3 (%)
Magnetic Susceptibility
Leg 165 Site 998A
Magnetic Susceptibility
160 80 0
120
130
140
150
160
170
180
Depth (mbsf)
Age (Ma)
CN9a
8.3
CN8
9.6
CN7
10.5
CN6
10.8
CN5
13.2
13.5
CN4/CN3
0 40 80
CaCO3 (%)
Caribbean (Yucatan Basin)
Waterdepth: 3101 m
Leg 154 Site 926A
Magnetic Susceptibility
40 20 0
190
200
210
220
230
240
250
260
270
Age (Ma)
CN9a
8.3
CN8
9.6
CN7
10.5
CN6
10.8
CN5
13.2
13.5
CN4
0 40 80
CaCO3 (%)
Eq. East Atl. Ceara Rise)
Waterdepth: 3598 m

Figure 7.

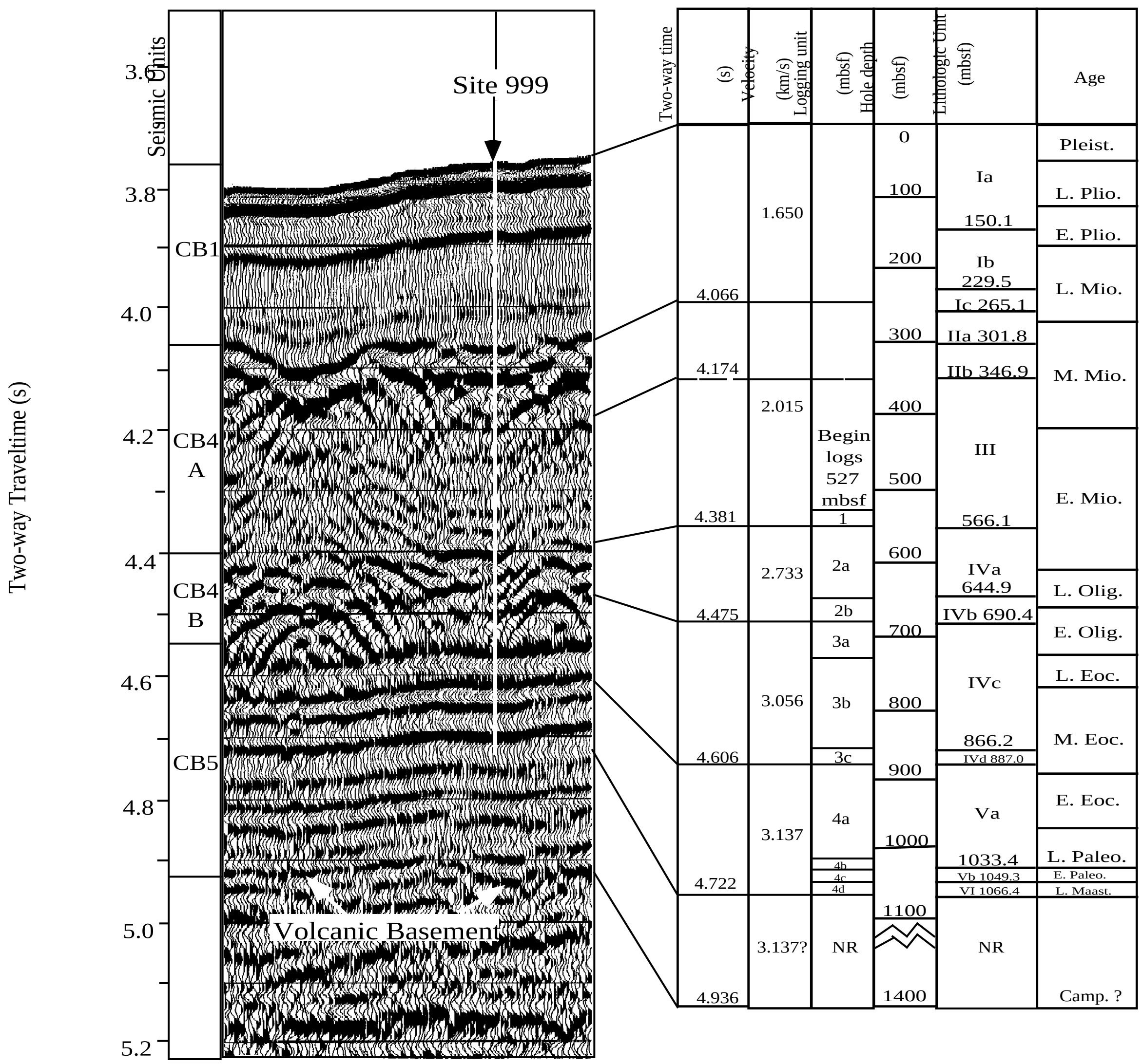
Two-way Traveltime (s)
Seismic Units
Site 999
3.6
3.8
4.0
4.2
4.4
4.6
4.8
5.0
5.2
CB1
CB4 A
CB4 B
CB5
Volcanic Basement
Two-way time (s)
Velocity (km/s)
Logging unit
Hole depth (mbsf)
Lithologic Unit (mbsf)
Age
4.066
4.174
4.381
4.475
4.606
4.722
4.936
1.650
2.015
2.733
3.056
3.137
3.137?
Begin logs 527 mbsf
1
2a
2b
3a
3b
3c
4a
4b
4c
4d
NR
0
100
200
300
400
500
600
700
800
900
1000
1100
1400
Ia
150.1
Ib
229.5
Ic 265.1
IIa 301.8
IIb 346.9
III
566.1
IVa
644.9
IVb 690.4
IVc
866.2
IVd 887.0
Va
1033.4
Vb 1049.3
VI 1066.4
NR
Pleist.
L. Plio.
E. Plio.
L. Mio.
M. Mio.
E. Mio.
L. Olig.
E. Olig.
L. Eoc.
M. Eoc.
E. Eoc.
L. Paleo.
E. Paleo.
L. Maast.
Camp. ?

Figure 8.

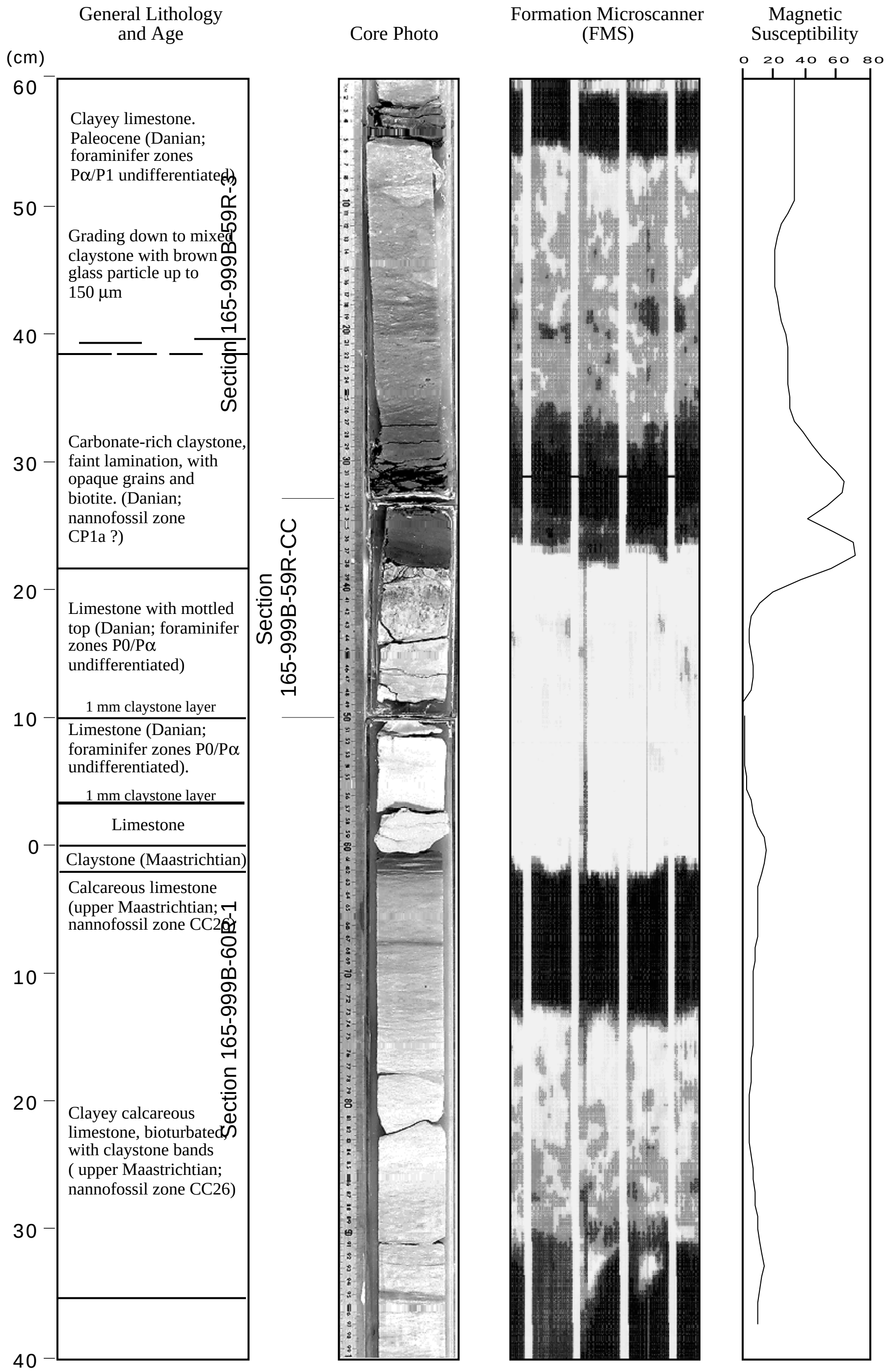
General Lithology and Age
Core Photo
Formation Microscanner (FMS)
Magnetic Susceptibility
(cm)
0 20 40 60 80
60
50
40
30
20
10
0
10
20
30
40
Clayey limestone. Paleocene (Danian; foraminifer zones Pα/P1 undifferentiated)
Grading down to mixed claystone with brown glass particle up to 150 µm
Carbonate-rich claystone, faint lamination, with opaque grains and biotite. (Danian; nannofossil zone CP1a ?)
Limestone with mottled top (Danian; foraminifer zones P0/Pα undifferentiated)
1 mm claystone layer
Limestone (Danian; foraminifer zones P0/Pα undifferentiated).
1 mm claystone layer
Limestone
Claystone (Maastrichtian)
Calcareous limestone (upper Maastrichtian; nannofossil zone CC26)
Clayey calcareous limestone, bioturbated with claystone bands (upper Maastrichtian; nannofossil zone CC26)
Section 165-999B-59R-3
Section 165-999B-59R-CC
Section 165-999B-60R-1

Figure 9.

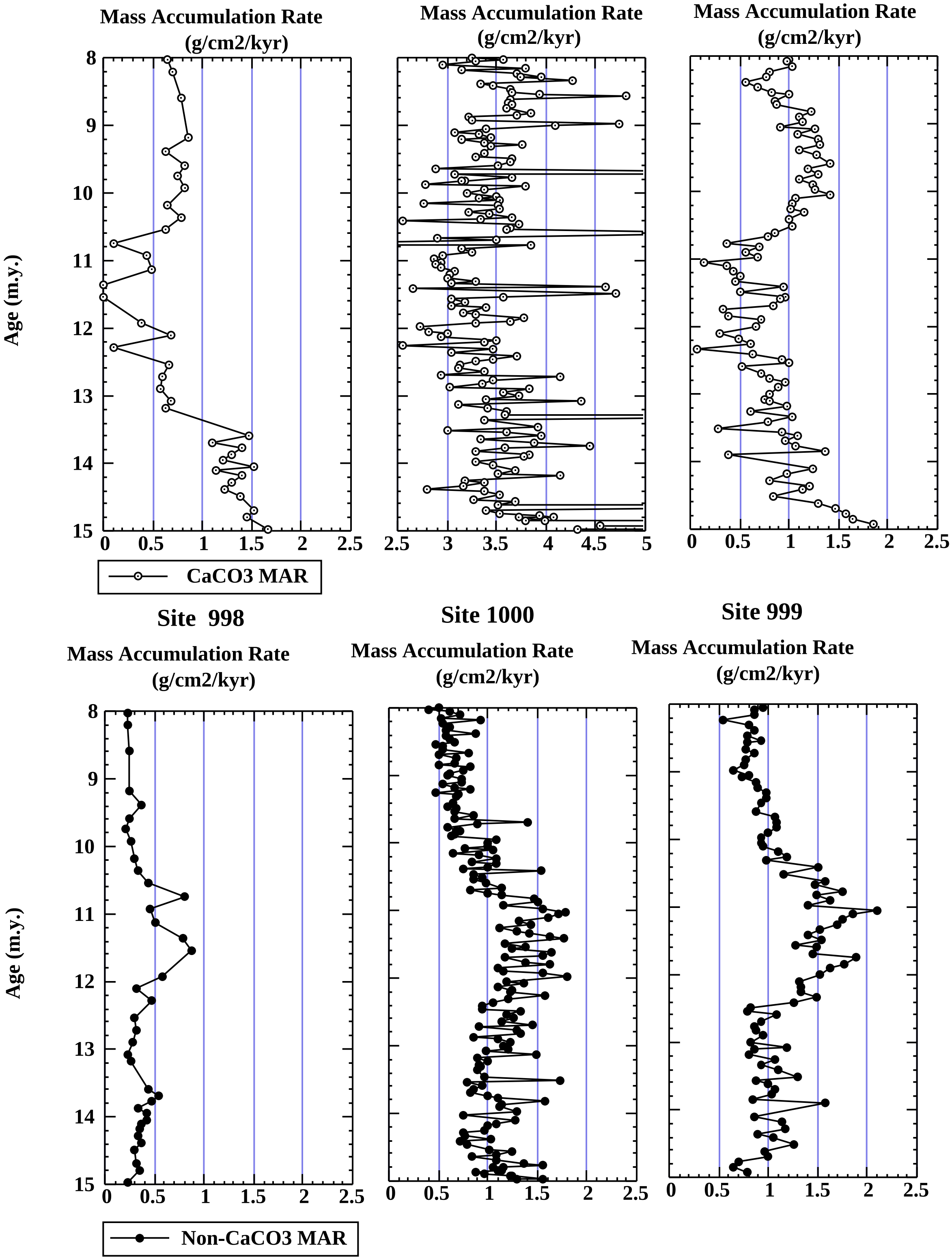
Mass Accumulation Rate (g/cm2/kyr)
Age (m.y.)
CaCO3 MAR
Site 998
Site 1000
Site 999
Mass Accumulation Rate (g/cm2/kyr)
Age (m.y.)
Non-CaCO3 MAR

Figure 10.

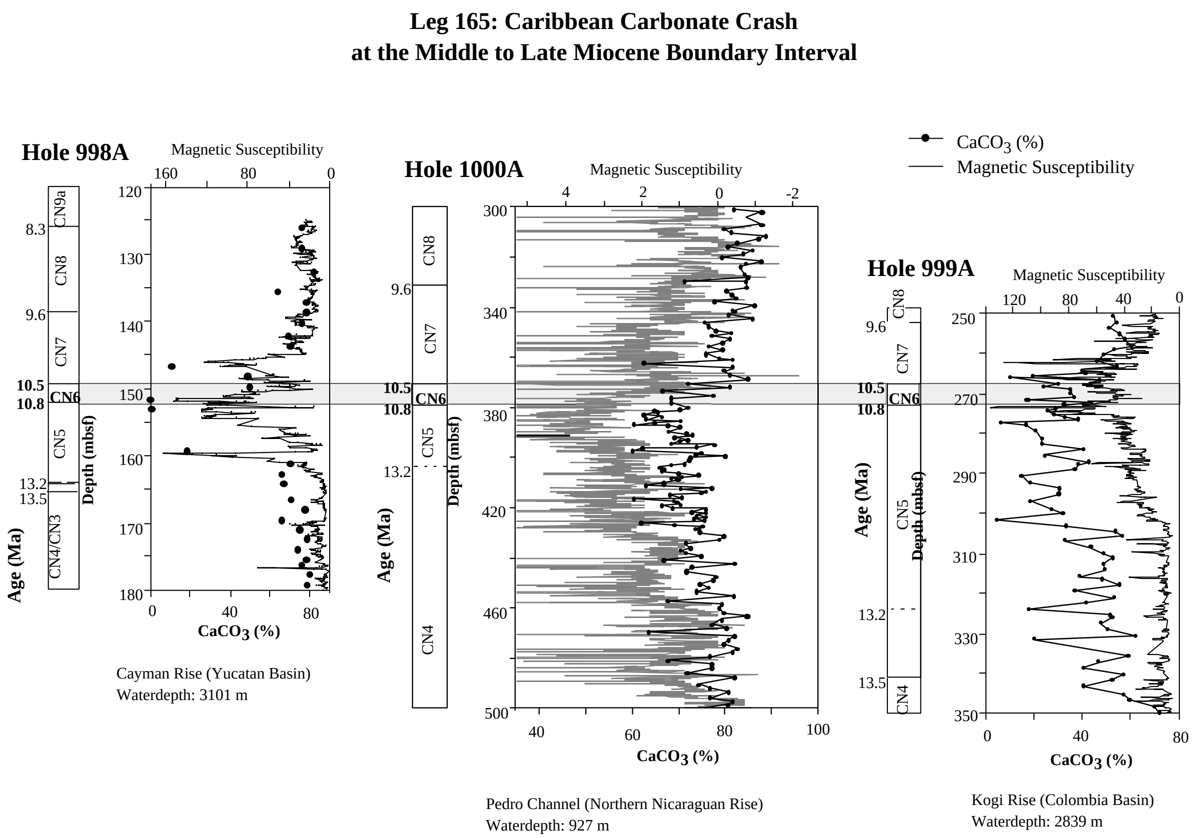
Leg 165: Caribbean Carbonate Crash
at the Middle to Late Miocene Boundary Interval
Hole 998A
Magnetic Susceptibility
Age (Ma)
Depth (mbsf)
CaCO3 (%)
Cayman Rise (Yucatan Basin)
Waterdepth: 3101 m
Hole 1000A
Magnetic Susceptibility
Age (Ma)
Depth (mbsf)
CaCO3 (%)
Pedro Channel (Northern Nicaraguan Rise)
Waterdepth: 927 m
Hole 999A
Magnetic Susceptibility
Age (Ma)
Depth (mbsf)
CaCO3 (%)
Kogi Rise (Colombia Basin)
Waterdepth: 2839 m
CaCO3 (%)
Magnetic Susceptibility
CN9a
CN8
CN7
CN6
CN5
CN4/CN3
CN4
8.3
9.6
10.5
10.8
13.2
13.5

Figure 11.

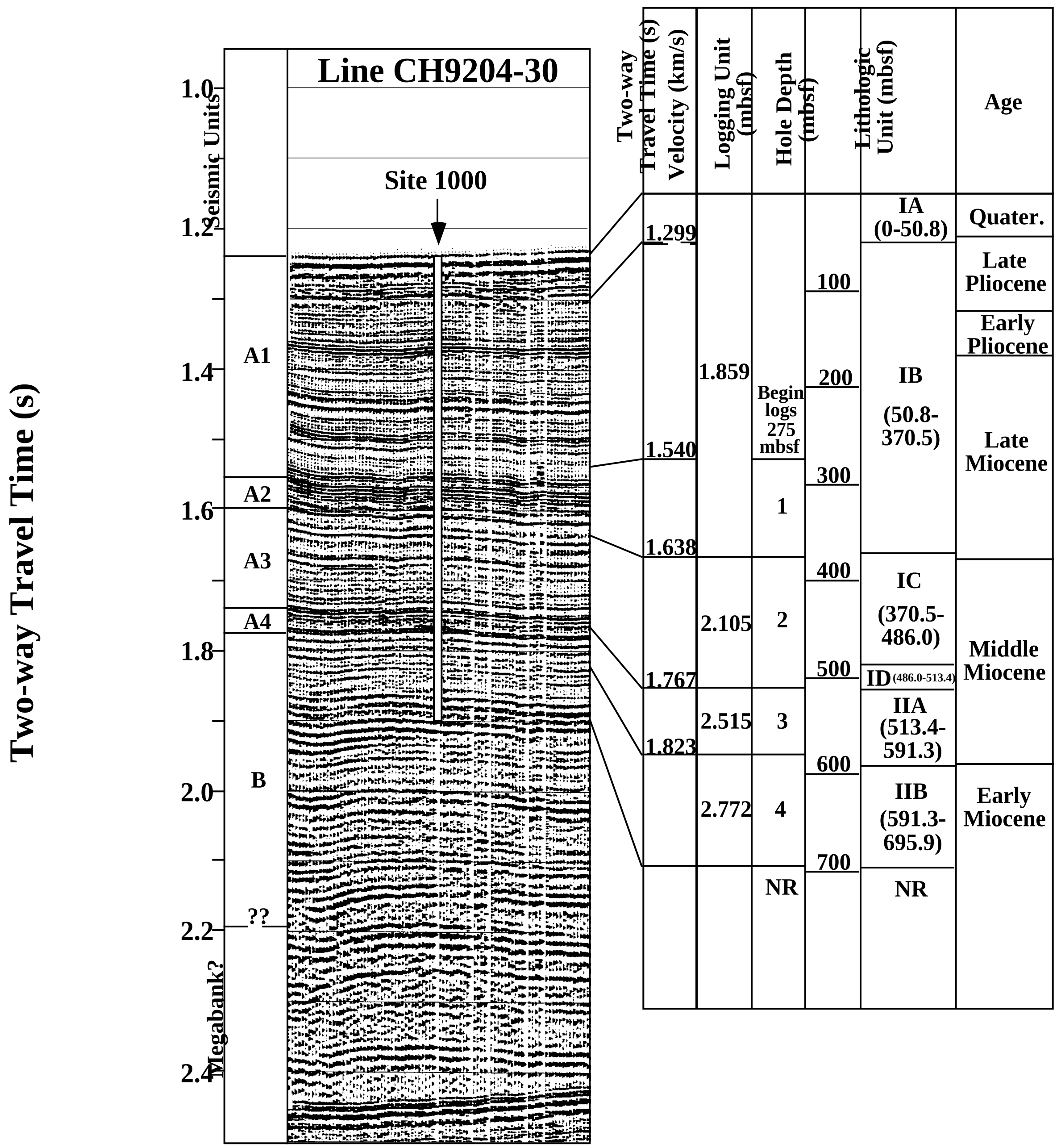
Two-way Travel Time (s)
1.0
1.2
1.4
1.6
1.8
2.0
2.2
2.4
Seismic Units
A1
A2
A3
A4
B
??
Megabank?
Line CH9204-30
Site 1000
Two-way Travel Time (s) Velocity (km/s)
1.299
1.540
1.638
1.767
1.823
Logging Unit (mbsf)
1.859
2.105
2.515
2.772
Hole Depth (mbsf)
Begin logs 275 mbsf
1
2
3
4
NR
100
200
300
400
500
600
700
Lithologic Unit (mbsf)
IA (0-50.8)
IB (50.8-370.5)
IC (370.5-486.0)
ID (486.0-513.4)
IIA (513.4-591.3)
IIB (591.3-695.9)
NR
Age
Quater.
Late Pliocene
Early Pliocene
Late Miocene
Middle Miocene
Early Miocene

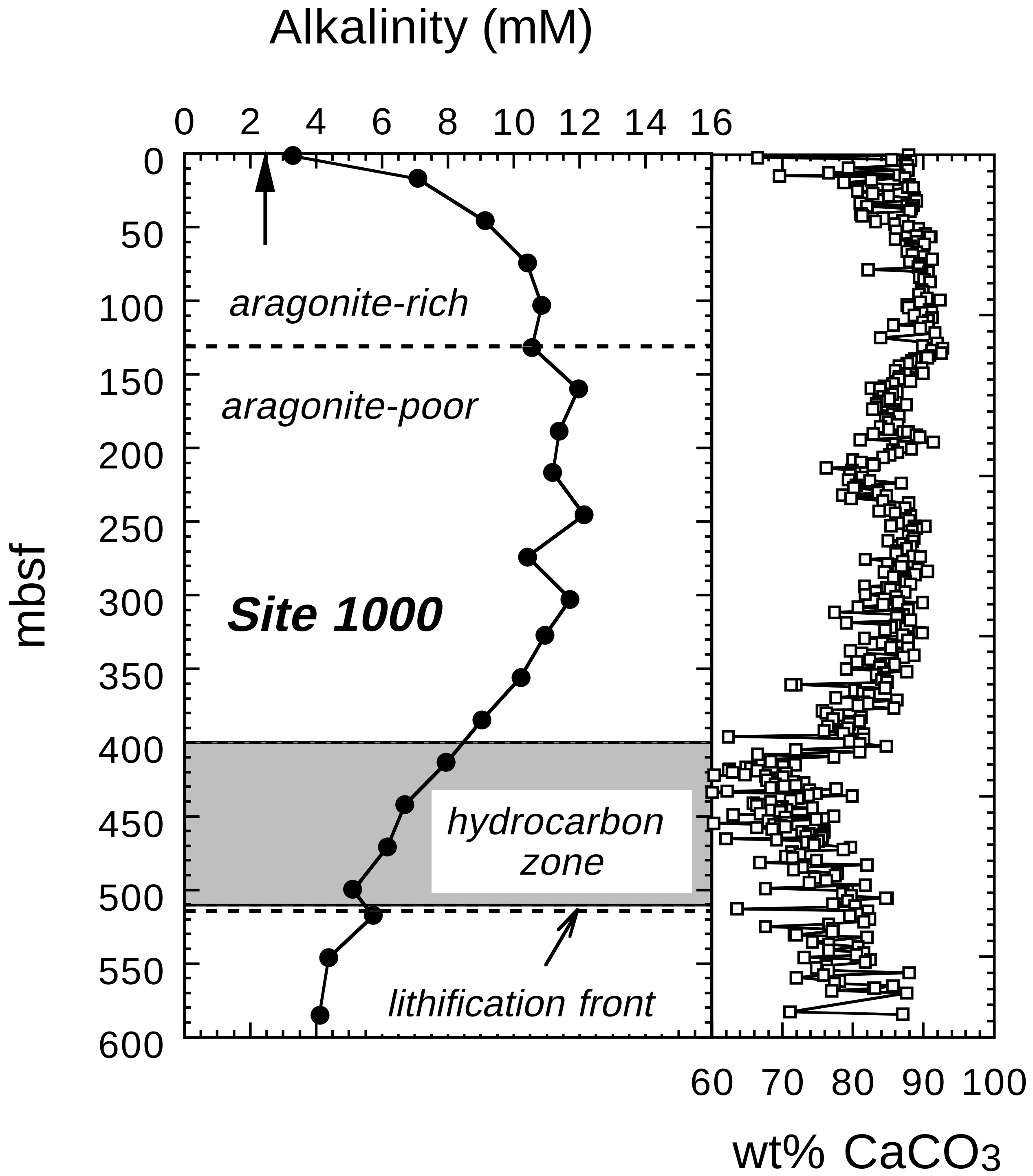
Alkalinity (mM)
0 2 4 6 8 10 12 14 16
mbsf
0
50
100
150
200
250
300
350
400
450
500
550
600
aragonite-rich
aragonite-poor
Site 1000
hydrocarbon zone
lithification front
60 70 80 90 100
wt% CaCO3

Figure 13.

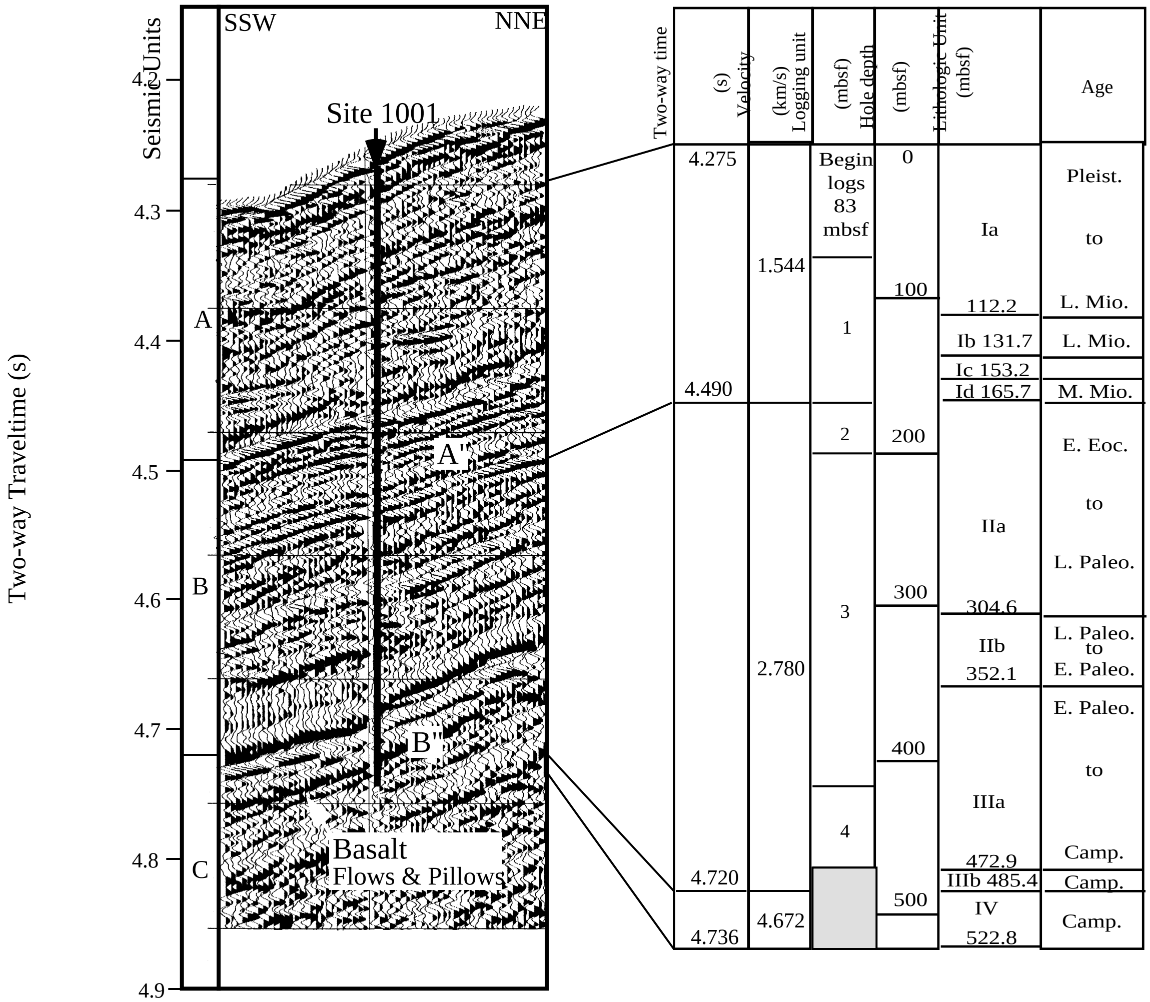
Two-way Traveltime (s)
Seismic Units
SSW
NNE
Site 1001
A
A"
B
B"
C
Basalt
Flows & Pillows
4.2
4.3
4.4
4.5
4.6
4.7
4.8
4.9
Two-way time (s)
Velocity (km/s)
Logging unit
Hole depth (mbsf)
(mbsf)
Lithologic Unit (mbsf)
Age
4.275
4.490
4.720
4.736
1.544
2.780
4.672
Begin logs 83 mbsf
1
2
3
4
0
100
200
300
400
500
Ia
112.2
Ib 131.7
Ic 153.2
Id 165.7
IIa
304.6
IIb
352.1
IIIa
472.9
IIIb 485.4
IV
522.8
Pleist.
to
L. Mio.
L. Mio.
M. Mio.
E. Eoc.
to
L. Paleo.
L. Paleo.
to
E. Paleo.
E. Paleo.
to
Camp.
Camp.
Camp.

Figure 14.

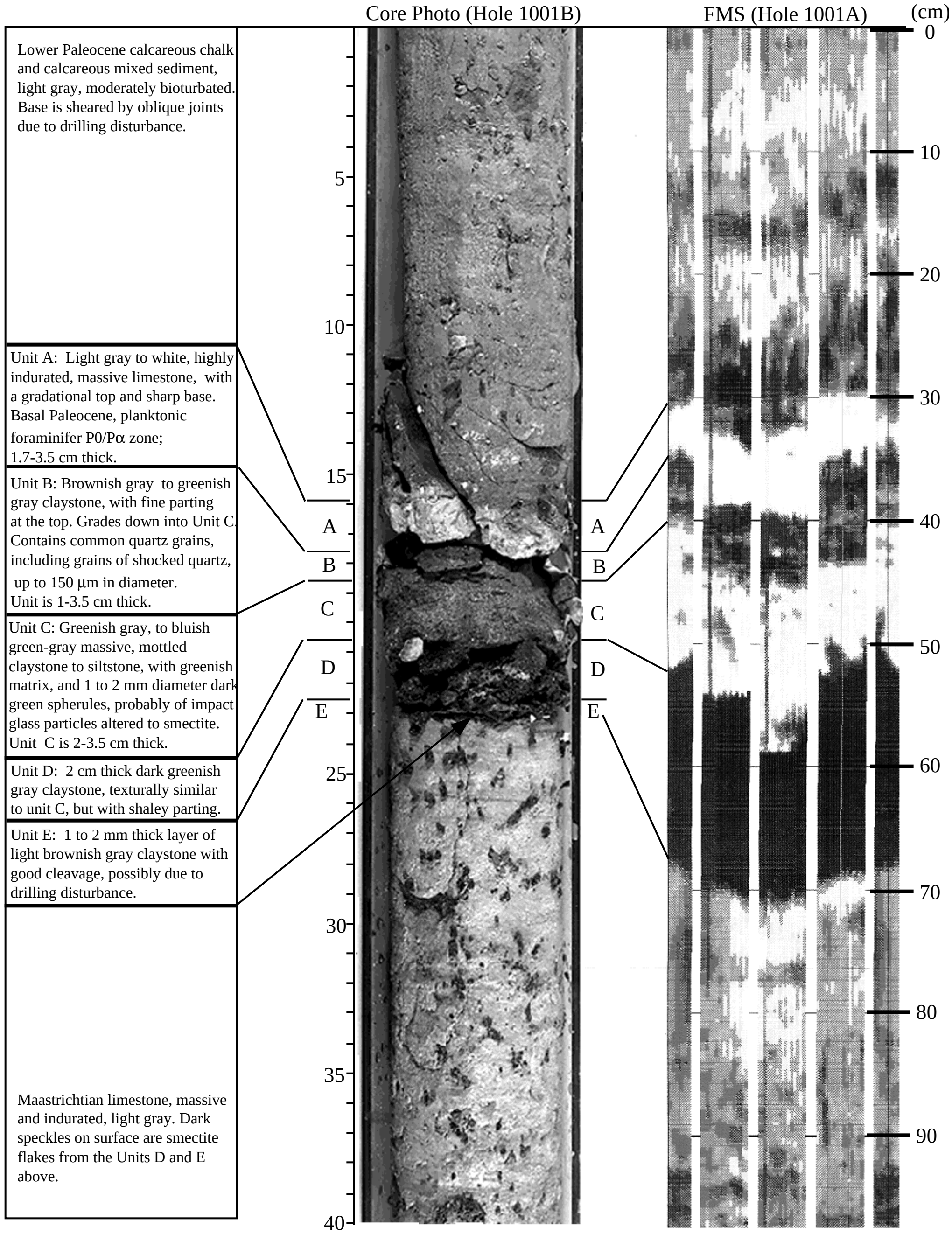
Core Photo (Hole 1001B)
FMS (Hole 1001A)
(cm)
Lower Paleocene calcareous chalk and calcareous mixed sediment, light gray, moderately bioturbated. Base is sheared by oblique joints due to drilling disturbance.
Unit A: Light gray to white, highly indurated, massive limestone, with a gradational top and sharp base. Basal Paleocene, planktonic foraminifer P0/Pα zone; 1.7-3.5 cm thick.
Unit B: Brownish gray to greenish gray claystone, with fine parting at the top. Grades down into Unit C. Contains common quartz grains, including grains of shocked quartz, up to 150 µm in diameter. Unit is 1-3.5 cm thick.
Unit C: Greenish gray, to bluish green-gray massive, mottled claystone to siltstone, with greenish matrix, and 1 to 2 mm diameter dark green spherules, probably of impact glass particles altered to smectite. Unit C is 2-3.5 cm thick.
Unit D: 2 cm thick dark greenish gray claystone, texturally similar to unit C, but with shaley parting.
Unit E: 1 to 2 mm thick layer of light brownish gray claystone with good cleavage, possibly due to drilling disturbance.
Maastrichtian limestone, massive and indurated, light gray. Dark speckles on surface are smectite flakes from the Units D and E above.
A
B
C
D
E
5
10
15
25
30
35
40
0
10
20
30
40
50
60
70
80
90

Figure 15.

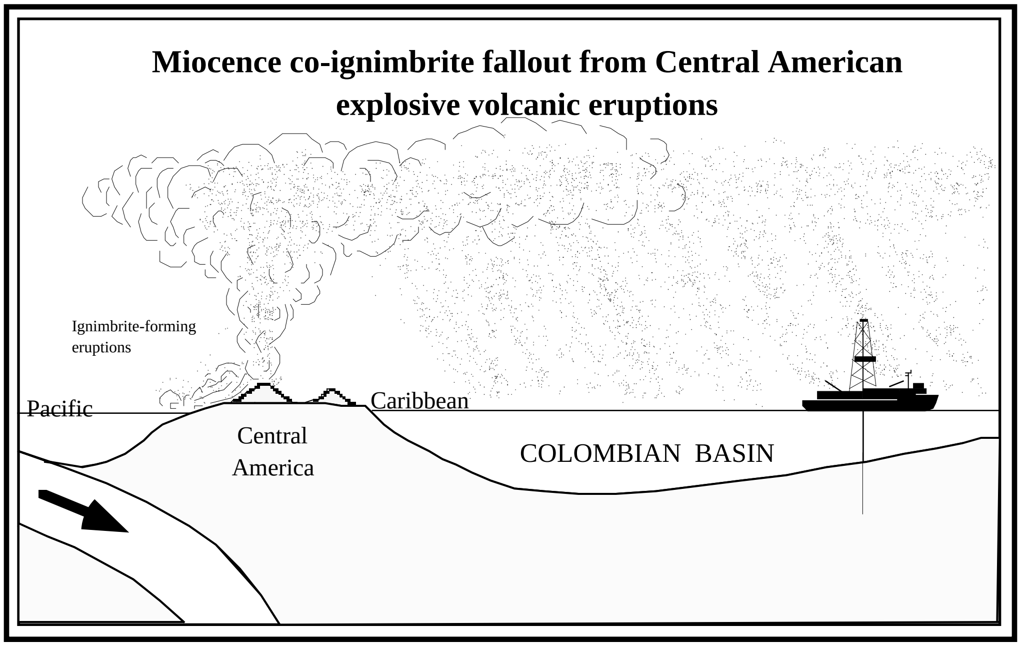
Miocence co-ignimbrite fallout from Central American explosive volcanic eruptions
Ignimbrite-forming eruptions
Pacific
Caribbean
Central America
COLOMBIAN BASIN

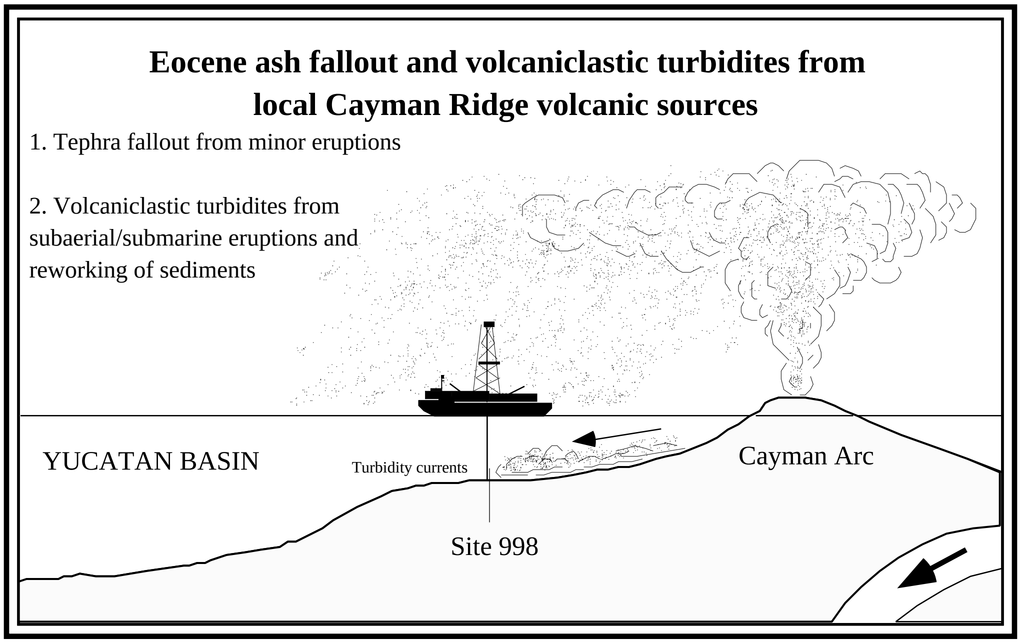
Eocene ash fallout and volcaniclastic turbidites from local Cayman Ridge volcanic sources
1. Tephra fallout from minor eruptions
2. Volcaniclastic turbidites from subaerial/submarine eruptions and reworking of sediments
YUCATAN BASIN
Turbidity currents
Cayman Arc
Site 998

Figure 16.

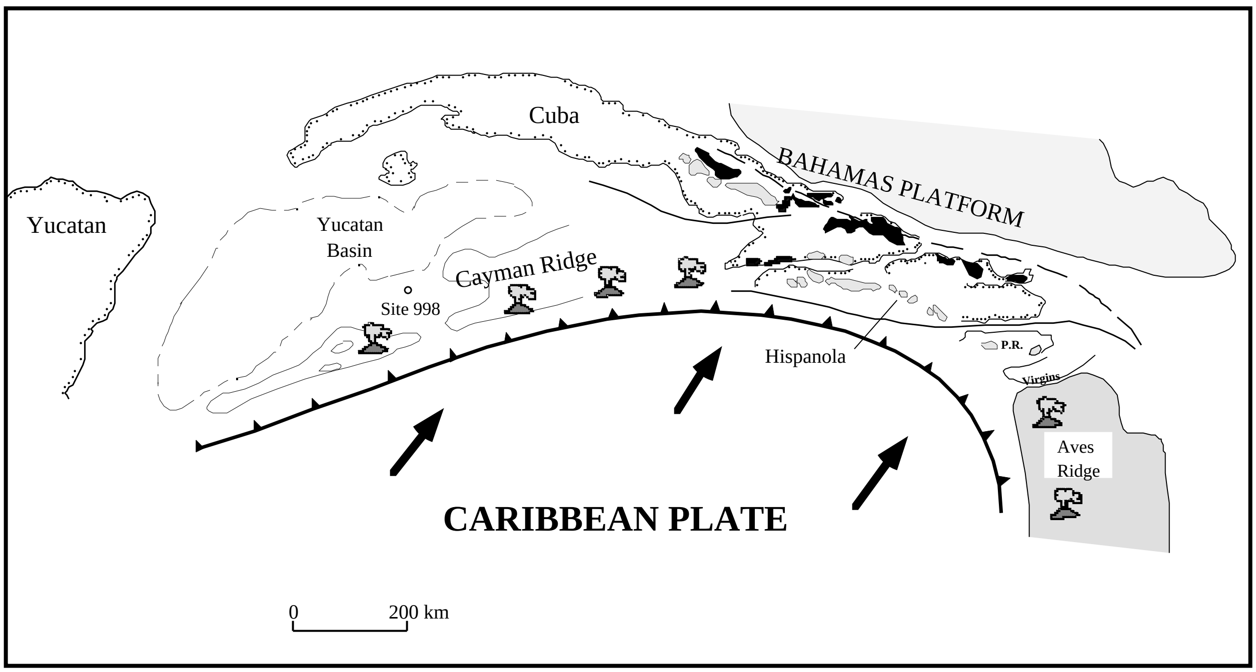
Cuba
BAHAMAS PLATFORM
Yucatan
Yucatan
Basin
Cayman Ridge
Site 998
Hispanola
P.R.
Virgins
Aves
Ridge
CARIBBEAN PLATE
0
200 km

OPERATIONS REPORT

The ODP Operations and Engineering personnel aboard *JOIDES Resolution* for Leg 165 were:

Operations Superintendent:	Michael Storms
Schlumberger Engineer:	Raymond Faust

Site 998

The 585 nmi transit from Miami was uneventful with calm seas and favorable currents. The ship proceeded at an average speed of 11.0 kt, dropping to a slightly lower speed of 8.25 kt while heading into the Gulf Stream current.

At Hole 998A, core recovery with the Advanced Piston Coring (APC) system was excellent (100%-107%). The Extended Core Barrel (XCB) coring system achieved good recovery (typically 60%-100%) and rate of penetration until the cutting shoe began to jam. Core quality also deteriorated with depth, though hole conditions remained excellent throughout the drilling.

Drilling at Hole 998B was initiated 20 m to the northeast of Hole 998A. The hole was drilled down to 558.5 mbsf with the Rotary Core Barrel (RCB) and center-bit combination before attempting core recovery. This depth was selected to allow about 80 m overlap of the lower, poorly recovered section of the formation from Hole 998A. Core recovery with the RCB was exceptionally good, averaging 83.1% for the hole.

Four suites of logging tools were deployed in the hole: The first two runs, with the Quad Combination tool and the Geochemical Logging tool, reached the bottom of the hole without incident and logged from 904 to 172 mbsf. Owing to an obstruction in the hole, the third and fourth runs, with the Formation MicroScanner and Geological High-Sensitivity Magnetic tool, only reached a total depth of 430 mbsf and logged up to 172 mbsf.

Site 999

The 468-nmi transit from Site 998 was slower than anticipated owing to the failure of a propulsion motor; this required that two motors be taken offline, which reduced average speed to about 10.7 kt.

Hole 999A was cored with the APC (average recovery 104.6%) and the XCB (89.0%) systems. The latter suffered from core biscuiting (a phenomenon in which the core is broken into many short cylindrical chunks that are surrounded by fine-grained drill cuttings and paste). Coring operations were terminated on this hole when the formation became indurated enough to provide an acceptable casing seat, which was then used in drill plans for Hole 999B, the reentry hole. Logging activities in Hole 999A were abandoned after the initial logging tool encountered an obstruction and then experienced repeated electrical failures.

The reentry cone and casing were installed in Hole 999B without incident. A CC-4 tungsten carbide roller cone insert bit was selected for RCB coring because the formation was expected to get progressively harder, eventually grading into silicified limestone and chert. The bit repeatedly clogged with aluminum debris from the cementing dart used in the casing installation, resulting in no core recovery for the first four cores. The debris was removed after tripping the drill string back to the surface, which resulted in a delay of ~14 hr. The rate of penetration (ROP) rapidly deteriorated with depth; the ROP for the last two cores was 3.2 m/hr and 2.4 m/hr, respectively, compared with 4.7 m/hr for the previous 100-m interval. At these rates we would not have been able to reach the depth objectives, and so a decision was made to switch to a PDC anti-whirl core bit. The bit change required another trip to the surface with the drill string, another reentry into the hole, and another ~15 hr delay.

The new PDC bit proved to be worth the extra time, as there was a slight improvement in core quality and a significant increase in the ROP, which averaged 8.9 m/hr over the first 100-m interval, or 2-4 times that achieved by the CC-4 bit. Even when the formation became a well-indurated limestone, the ROP only dropped to 6.9 m/hr for the PDC bit.

The ROP only began to decrease significantly at a depth of about 1046 mbsf, during coring of 165- 999B-59R, which was also marked by an increase in drill pump pressure from 500 psi to about 750 psi. Core 165-999B-59R was thought to be the core that would contain the K/T boundary interval. Our primary concern was that the increased pump pressures would wash away part or all of the critical interval, and thus a joint decision was made to retrieve the core after advancing only 4.6 m. The ROP dropped even farther, to about 1.5 m/hr, during coring of the next three cores (165-999B-60R through 62R), which indicated bit degradation. Perhaps due to luck, or to the extra care taken while drilling through the critical interval, the overall recovery (92.9%) for the last four cores was over 10% higher than achieved for the other part of the hole cored with the PDC bit.

Having determined that we were about 15 m into the Upper Cretaceous section and realizing that further coring at the very slow ROP would gain us little given the time constraints, we ended coring operations at a depth of 1066.4 mbsf. The hole was then prepared for logging with sepiolite mud sweeps without using a wiper trip. Hole conditions were excellent for logging, which resulted in smooth logging operations and high quality Quad Combo, Geochemical Logging Tool, and Formation Microscanner logs.

Site 1000

Before heading to Site 1000 from Site 999 we docked in Kingston, Jamaica, to take aboard a Honduran observer and a scientist from the JOIDES office in Cardiff, to load propulsion motors and freight, and to disembark the Colombian observer/scientist and a scientist (who left for medical reasons). The 550-nmi transit from Kingston to Site 1000 was covered at an average speed of 9.6 kt.

Hole 1000A was cored with the APC and XCB systems. Owing to the thick section of unconsolidated and poorly indurated sediments, we were able to recover 34 APC cores, which gave a 103.5% recovery for the interval from 0.0 to 312.9 mbsf. Two cores (165-1000A-10H and 13H) were highly disturbed upon recovery, possibly because the flapper on the core catcher may not have fully opened, thus forcing the core material to flow past the flapper. These intervals were later successfully recovered with the RCB system in Hole 1000B. The XCB system performed with high rates of penetration (ROP) and high recovery (86.5 m/hr with 100% recovery to 400 mbsf, 72.2 m/hr with 100.3% recovery to 500 mbsf, and 49.4 m/hr with 98.6% recovery to 525 mbsf) until a depth of 524 mbsf (Core 56X). Owing to poor recovery and a slow ROP on the next three cores, drilling was halted in Hole 1000A.

Hole 1000B was spudded about 30 m to the southwest of Hole 1000A with the RCB system. The hole was drilled ahead to 79.3 mbsf and then Core 165-1R was recovered in roughly the same interval as the disturbed Core 165-1000A-10H. It was decided to drill ahead to 117.3 mbsf and take Core 165-1000B-2R in roughly the same interval as the disturbed Core 165-1000A-13H. The hole was then drilled ahead to 503.5 mbsf where continuous RCB coring was initiated. Overall core recovery for Hole 1000B averaged 67.6%. Coring ceased at a depth of 695.9 mbsf due to time constraints, and the hole was prepared for logging operations. Quad Combo, Geological High-Sensitivity Magnetic, and Formation MicroScanner logs were acquired in Hole 1000B.

Site 1001

Even with all propulsion motors back on line, the brisk trade winds slowed the vessel to an average speed of 10.1 kt on the 291-nmi transit from Site 1000. We arrived on site early Friday morning, 2 February 1996, to begin drilling operations.

Hole 1001A was spudded and cored with the RCB system, because the primary objectives was to acquire lithified rocks below a suspected abbreviated Neogene section and because there was insufficient time to piston core the unlithified sediments and then spud another hole with the RCB system. We used the subsea video camera as an aid to observe the bit contact with the seafloor and to obtain a mudline core. This accurately defined the water/seafloor interface, though only a small piece of ooze was recovered in Core 165-1001A-1R. Core recovery varied between 0.5% and 22% for the first six cores. Recovery for Cores 11R through 18R ranged from 80% to 102%, but dropped off rapidly after a major unconformity was encountered at 165.68 mbsf (at Section 165-1001A-18R-4, 88 cm), where middle Miocene ooze overlies middle and lower Eocene chalk and limestones with numerous, thin chert layers. Recovery through the hard limestones and chert ranged from 0% to 57%, but improved significantly below 303 mbsf where the chert layers were absent to very sparse. Some of the highest recovery intervals were at the K/T boundary (Core 165-1001A-38R) and at the basement contact (Core 165-1001A-52R), the latter of which was of exceptionally good quality.

Coring ceased in Hole 1001A after cutting four cores below the basement contact. The hole was circulated clean and a wiper trip was made to 112 mbsf in preparation for logging operations. Quad Combo, Formation MicroScanner, Geological High-Sensitivity Magnetic logs were acquired in Hole 1001A.

Hole 1001B is located approximately 15 nmi to the south of Hole 1001A. Two spot RCB cores were collected, at 25.3 and 150.3 mbsf, as the hole was being drilled down to 206.5 mbsf, where continuous coring operations began. In general, core recovery matched that from Hole 1001A for similar depth intervals. The interval cored, however, was offset by 2 m in depth from that of Hole 1001A in hope of recovering the intervals missed in Hole 1001A, and to position the K/T boundary interval within the core liner, rather than in the core catcher. This strategy was successful as we not only collected the K/T boundary where planned, but also managed to recover another Paleocene/Eocene boundary section and another basement/sediment contact. Coring ceased at a depth of 488.3 mbsf (2 m into basement) due to time constraints.

Site 1002

The 635-nmi transit from Site 1001 was made at an average speed of 10.5 kt. While the ship was on route to the site, two Venezuelan observers arrived by helicopter, and the Honduran observer and the JOIDES scientist departed. A short site survey was conducted with the 3.5-Hz echo-sounder on approach to the site to verify that the site was properly located on the proposed local topographic high. Five holes were drilled, with each hole being offset by about 15 m east of the previous hole.

Hole 1002A was spudded with the APC system at 0.7 mbsf. The core liner was full (102.7% recovery), but did not contain a mudline, which necessitated spudding Hole 1002B, because the shipboard geochemists needed a mudline core for their proposed interstitial water studies. Hole 1002B recovered 6.2 m of sediment, including the mudline.

The APC system performed well, with 109.1% average recovery for the hole. Cores 12H-18H suffered from flow-in disturbance in the lower 2 to 3 m of each core. The liner for Core 165-1002C-18H was severely damaged and the core had to be pumped out of the core barrel, though 9.92 m of sediment was still recovered. Core 165-1002C-19H also returned to the surface shattered, but this time only 0.15 m of sediment and hard dolomite was recovered.

The APC/XCB coring systems were used for Holes 1002D and E. Hole 1002D was spudded with the drill string 3 m higher than that used at Hole 1002C, and Hole 1002E was offset another 3 m, to offset core breaks. The XCB system was used after Core 12H for Hole 1002D and after Core 13H for 1002E to avoid the flow-in problem and to penetrate the dolomite lenses more easily. Recovery was very good for both holes, averaging over 105% for the APC portions and over 70% for the XCB portions. Coring operations for both holes were halted just above the hard dolomite encountered in Core 165-1002C-19H to avoid penetrating any potentially dangerous gas pockets.

ODP LEG 165

OPERATIONS SUMMARY

Total Days (19 December 95 to 17 February 96)	60.2
Days in Port	2.9
Days Underway	12.7
Days On-Site	44.7
Coring	26.9
Repair Time (ODP)	0.1
Tripping	7.3
Logging/Downhole Science	4.5
Drilling	2.4
Other	2.4
Casing and Cementing	1.0
Stuck Pipe/Downhole Trouble	0.0
Development Engineering	0.0
Repair Time (Contractor)	0.0
W.O.W.	0.0
Fishing & Remedial	0.0
Total Distance Traveled (nautical miles)	3084
Total Miles Transited:	3047
Average Speed Transit (knots):	10.3

Total Miles Surveyed:	37
Average Speed Survey (knots):	5.0
Number of Sites	5
Number of Holes	13
Total Interval Cored (m)	4178.4
Total Core Recovery (m)	3358.82
% Core Recovery	80.4
Total Interval Drilled (m)	1774.0
Total Penetration (m)	5952.4
Maximum Penetration (m)	1066.4
Maximum Seafloor Depth (meters from drilling datum)	3271.0
Minimum Seafloor Depth (meters from drilling datum)	904.1

OCEAN DRILLING PROGRAM

SITE SUMMARY

LEG 165

Hole	Latitude	Longitude	Sea-floor Depth (mbrf)	Total No. Cores	Total Interval Cored (meters)	Total Core Recovered (meters)	Average Percent Recovered (percent)	Total Interval Drilled (meters)	Sub-Bottom Depth (mbsf)	Total Time On Hole (hours)	Total Time On Hole (days)
998A	19° 29.377'	82° 56.166'	3190.7	67	637.6	440.89	69.10	0	637.6	111	4.63
998B	19° 29.387'	82° 56.166'	3190.7	37	346.5	287.9	83.10	558.3	904.8	258	10.75
			S-2B Site Totals:	104	984.1	728.79	74.10	558.3	1542.4	369	15.38
999A	12° 44.639'	78° 44.360'	2838.9	61	566.1	534.73	94.50	0	566.1	99.75	4.16
999B	12° 44.597'	78° 44.418'	2838.9	62	523	397.89	76.10	543.4	1066.4	348.75	14.53
			S-6 Site Totals:	123	1089.1	932.62	85.60	543.4	1632.5	448.5	18.69
1000A	16° 33.223'	79° 52.044'	927.2	59	553.2	538.28	97.30	0	553.2	42.5	1.77
1000B	16° 33.219'	79° 52.046'	927.2	22	211.4	142.97	67.60	484.5	695.9	71.75	2.99
			NR-1/2 Site Totals:	81	764.6	681.25	89.10	484.5	1249.1	114.25	4.76
1001A	15° 45.427'	74° 54.627'	3271	56	522.8	286.23	54.70	0	522.8	136.75	5.7
1001B	15° 45.418'	74° 54.626'	3271	32	301.2	201.14	66.80	187.1	488.3	72.75	3.03
			S-3B Site Totals:	88	824	487.37	59.10	187.1	1011.1	209.5	8.73
1002A	10° 42.366'	65° 10.179'	904.3	1	9.5	9.77	102.80	0.7	10.2	4.25	0.18
1002B	10° 42.366'	65° 10.179'	904.3	1	6.2	6.24	100.60	0	6.2	0.5	0.02
1002C	10° 42.368'	65° 10.166'	904.1	19	170.1	185.71	109.20	0	170.1	12	0.5
1002D	10° 42.368'	65° 10.161'	904.8	18	166.8	162.19	97.20	0	166.8	12.75	0.53
1002E	10° 42.364'	65° 10.155'	904.7	18	164	164.88	100.50	0	164	14.25	0.59
			CB-1A Site Totals:	57	516.6	528.79	102.40	0.7	517.3	43.75	1.82
			Leg 165 Grand Totals:	453	4178.4	3358.82	80.40	1774	5952.4	1185	49.38

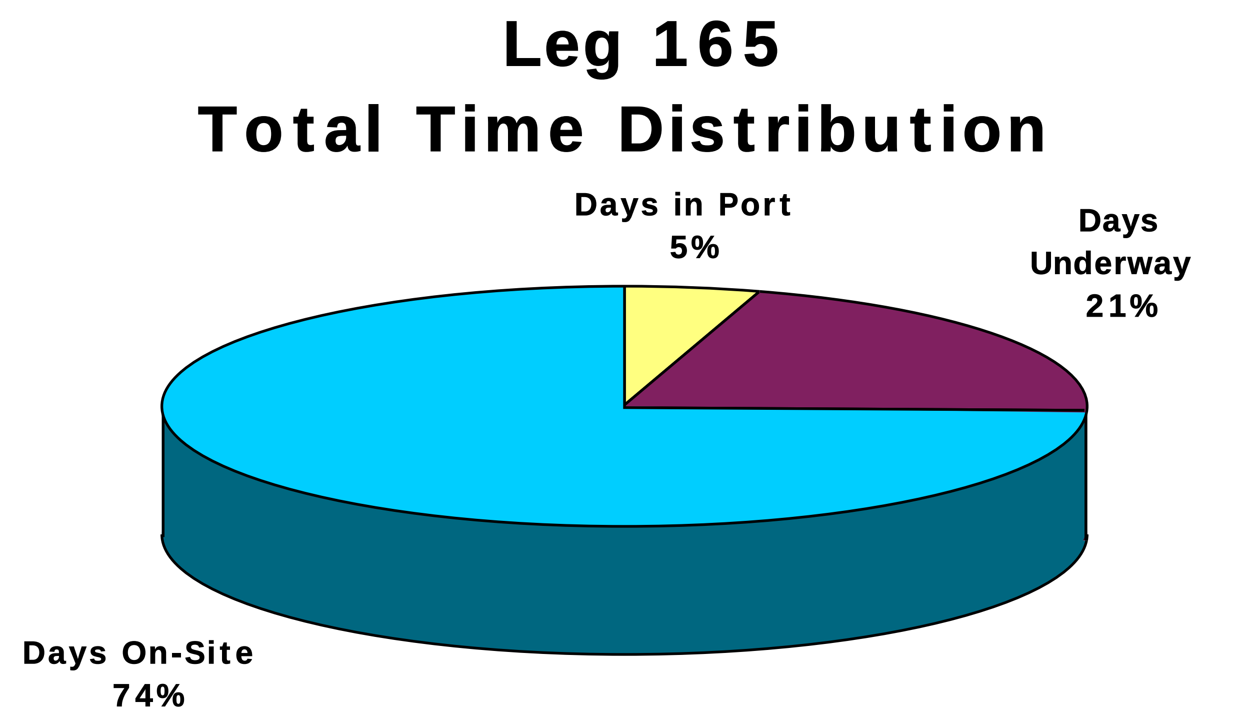
Leg 165
Total Time Distribution
Days in Port
5%
Days
Underway
21%
Days On-Site
74%

TECHNICAL REPORT

The ODP Operations and Engineering personnel aboard *JOIDES Resolution* for Leg 165 were:

John Dyke	Marine Lab Specialist (Store Keeper)
Tim Fulton	Marine Lab Specialist (Photographer)
Edwin Garrett	Marine Lab Specialist (Paleomagnetics)
Dennis Graham	Marine Lab Specialist (Chemistry)
“Gus” Gustafson	Marine Lab Specialist (Downhole/Thin Section)
Burney Hamlin	Laboratory Officer
Michiko Hitchcox	Marine Lab Specialist (Yeoperson)
Terry Klepak	Marine Computer Specialist
John Lee	Marine Lab Specialist (Chemistry)
Kevin MacKillop	Marine Lab Specialist (Physical Properties)
Matt Mefferd	Marine Computer Specialist
Eric Meissner	Marine Electronics Specialist
Dwight Mossman	Marine Electronics Specialist
Scott Rutherford	Marine Lab Specialist
Don Sims	Marine Lab Specialist (X-ray)
Lorraine Southey	Marine Lab Specialist (Curatorial)
Joel Sparks	Marine Lab Specialist (X-ray)

Port Call in Miami, Florida

The technical staff supporting Leg 165 began crossover activities with the Leg 164 technical staff on the morning of 19 December 1995 in Miami, Florida. The two technical teams continued until 1300 hrs, when a Texas A&M mandatory annual Radiation Safety seminar was conducted by Kieth Carsten. Other port activities included the installation of the new DEC AlphaServer, which is central to the JANUS installation, and refilling the cryogenic magnetometer with liquid helium.

The ship sailed at 2030 hr, on 21 December, approximately an hour after the last scientist arrived aboard. Leaving with us, besides the routine complement of personnel, were two TRACOR representatives, to test modules of the JANUS database with the newly installed system server, and an observer representing Colombia, as the second site would be in Colombian waters. The early departure added valuable time to the tight time schedule of Leg 165.

Underway

Navigation tapes and depth recorders were turned on as the ship left Miami, and the magnetometer sensor was deployed west of Key West when the ship's course lay outside the coastal ship traffic and led into deeper water. The only seismic survey of the leg was at Site 999, where a 4-hr survey was conducted using two 200-in^3 HAMCO water guns. Strong trade winds and cross seas contributed to noisy analog records reflecting the sea state, as did the low filter settings selected, though subsequent processing improved the record considerably.

On the way to San Juan from Site 1002, the ballasted digital streamer was towed at various speeds and cable lengths to determine to what depth it would settle. The depth meter readings froze about two-thirds of the way through the planned stations and the test was canceled.

Special Objectives

The shallow-water piston coring and high-resolution water chemistry planned for the last site in the Cariaco Basin presented a challenge in planning and execution. This anoxic site is thought to retain the best climate record in the Atlantic for the past quarter of a million years, revealed by annual layering. All participants watched a hydrogen sulfide safety video early in the leg, and a meeting was held prior to arrival at the site to familiarize the party with the problems encountered recovering gassy sediments when high pressure or H_2S conditions are encountered. Temporary powered fume extractors were connected to the cutting room natural vent and one of the port holes. Hydrogen sulfide gas levels remained low with a peak of 7 ppm analyzed from one void in a core. Core lab condition were measured at 1 ppm maximum.

Curation

The leg presented a wide range of recovery, from the rapidly moving shallow-water multiple piston coring sites with gassy and anoxic muds through indurated carbonates and limestones to basement basalts. Critical K/T and Paleocene/Eocene boundaries and a record number of ash layers were recovered. Routinely recovered core was sent to the Bremen core repository (BCR). The critical K/T boundary and all the Cariaco cores, including unsplit cores from two holes, and BCR container core box overflow were sent to the Gulf Coast core repository for special attention, further sampling, and temporary storage.

Computer Services

Tracking and billing for personal cc:mail services was initiated on this leg. Weekly summaries were posted to keep people aware of their position in relation to the gratis allotment.

TRACOR initiated CORELOG and SAMPLE portions of the new JANUS database. The new server loaded, processed, and plotted MST data, while still being debugged by TRACOR and evaluated by the scientists. The core log portion of the JANUS system is now mostly functional.

Leg 165 Laboratory Statistics

General

Sites:	5
Number of Cores :	453
Number of Samples, Total	19,281
Number of Core Boxes	497

Magnetics Lab

Half section measurements :	2126
Discrete measurements:	334

Physical Properties

Index properties:	1855
Velocity :	1838
Resistivity:	451
Therm con:	176
MST:	2702
Shear Strength:	272

Chemistry Lab

Inorganic Carbonates (CACO3):	1795

Water Chemistry (the suite includes pH, Alkalinity, Sulfate, Chlorinity, Silica, Phosphate, Ammonia,

Ca, Mg, P, Li, Mn, Fe, Sr, Rb):	175

Head Space gas analysis:	356
Pyrolysis Evaluation, Rock-Eval :	12
X-ray Lab	
XRD :	257
XRF:	84 ash/basalt
	195 sediment
Thin Sections:	99
Underway Geophysics (est.)	
Total Transit Nautical Miles:	3079
Bathymetry:	2565
Magnetics:	2290
XBT's Used:	53